ANALYTICAL AND NUMERICAL INVESTIGATION OF UNIFORMLY LOADED SIMPLY SUPPORTED CIRCULAR PLATES

A THESIS SUBMITTED TO

THE GRADUATE SCHOOL OF NATURAL AND APPLIED SCIENCES

OF

ATILIM UNIVERSITY

BY

AQEEL NAJDET NASRET CORAN

IN PARTIAL FULFILLMENT OF THE REQUIREMENTS FOR THE DEGREE OF

MASTER OF SCIENCE

IN

THE DEPARTMENT OF CIVIL ENGINEERING

SEPTEMBER 2014

Approval of the Graduate School of Natural and Applied Sciences, Atılım University.

_____

Prof. Dr. İbrahim Akman
Director

I certify that this thesis satisfies all the requirements as a thesis for the degree of Master of Science.

_____

Assoc. Prof. Dr. Tolga Akış
Head of Department

This is to certify that we have read the thesis "Analytical and Numerical Investigation of Uniformly Loaded Simply Supported Circular Plates" submitted by Aqeel Najdet Nasret Coran and that in our opinion it is fully adequate, in scope and quality, as a thesis for the degree of Master of Science.

_____

Assoc. Prof. Dr. Tolga Akış
Supervisor

Examining Committee Members

Assoc. Prof. Dr. Hakan Argeşo _____
Manuf. Eng. Dept., Atılım University

Assoc. Prof. Dr. Tolga Akış _____
Civil Eng. Dept., Atılım University

Asst. Prof. Dr. H. Cenan Mertol _____
Civil Eng. Dept., Atılım University

Date: September 12, 2014

I declare and guarantee that all data, knowledge and information in this document has been obtained, processed and presented in accordance with academic rules and ethical conduct. Based on these rules and conduct, I have fully cited and referenced all material and results that are not original to this work.

Name, Last name : Aqeel Najdet Nasret Coran

Signature :

ABSTRACT

ANALYTICAL AND NUMERICAL INVESTIGATION OF UNIFORMLY LOADED SIMPLY SUPPORTED CIRCULAR PLATES

Aqeel Najdet Nasret Coran

M.S., Civil Engineering Department

Supervisor: Assoc. Prof. Dr. Tolga Akış

September 2014, 58 pages

Simply supported circular plates under uniform loading are investigated by analytical and numerical methods in this study. The stress, strain and displacement expressions are derived for the plates using the analytical methods based on (a) theory of elasticity approach, and (b) small displacement theory of thin plates. In addition to these, the numerical solution of the problem based on finite element method is obtained by using SAP 2000 software package. Finally, the results obtained by the analytical methods for different plate thicknesses are compared with each other and with the solutions obtained by the finite element method.

Key words: Stress Analysis; Stress Function; Thin and Thick Circular Plate

ÖZ

DÜZGÜN YAYILI YÜK ALTINDAKİ BASİT MESNETLİ DAİRESEL PLAKLARIN ANALİTİK VE SAYISAL YÖNTEMLERLE İNCELENMESİ

Aqeel Najdet Nasret Coran

Yüksek Lisans, İnşaat Mühendisliği Bölümü

Tez Danışmanı: Doç. Dr. Tolga Akış

Eylül 2014, 58 sayfa

Bu çalışmada düzgün yayılı yük taşıyan basit mesnetli dairesel plaklar analitik ve sayısal yöntemlerle incelenmiştir. Plaklarda (a) Elastisite Teorisi yaklaşımı ve (b) ince plaklar için Küçük Deplasman Teorisi metodları kullanılarak gerilme, birim şekil değiştirme ve yer değiştirme ifadeleri türetilmiştir. Bunlara ek olarak SAP 2000 yazılım paketi kullanılarak, sonlu eleman metodu temelinde problemin sayısal çözümü elde edilmiştir. Son olarak, farklı plak kalınlıkları için elde edilen analitik çözümler birbirleriyle ve sonlu eleman metodu sonuçlarıyla karşılaştırılmıştır.

Anahtar Kelimeler: Gerilme Analizi; Gerilme Fonksiyonu; İnce ve Kalın Dairesel Plak

To My Family

ACKNOWLEDGEMENTS

I am deeply heartened and thankful to my advisor, Assoc. Prof. Dr. Tolga Akış, for his guidance and support. It is impossible to have completed this work without his mentoring and support. I am short of words to express my gratitude to him. To my wife, Zainab, I offer sincere thanks for her continuous encouragement and patience during this period. And to my parents and brother, who gave their constant love and support for my whole life, I am grateful for helping me becoming who I am.

TABLE OF CONTENTS

LIST OF TABLES

LIST OF FIGURES

LIST OF SYMBOLS

r , θ, z	cylindirical polar coordinates
a	radius of circular plate
E	modulus of elastcity
ν	Poisson's ratio
u	radial displacement
w	transverse deflection
ϵ_r	radial strain
ϵ_θ	tangential strain
ϵ_z	strain in z-direction
γ_{rz}	shear strain
σ_r	radial stress
σ_θ	tangential stress
σ_z	stress in z-direction
τ_{rz}	shear stress
h	thickness of the plate
p	transverse uniform load
G	modulus of rigidity
N	horizontal force at the edge
M	moment at the edge
ϕ , ω	stress function

CHAPTER I

INTRODUCTION

1.1 General

Plate is a plane surface structure whose thickness is small compared to its other dimensions. Geometrically, they are bounded either by straight or curved lines. Plates have free, simply supported, and fixed boundary conditions, including elastic and plastic supports and restraints, or in some cases, point supports.

They are widely used in engineering structures, such as in architectural structures, bridges, hydraulic structures, pavements, containers, airplanes, missiles, ships, instruments and machine parts. Circular plates are common in many structures such as nozzle covers, end closures in pressure vessels, pump diaphragms, turbine disks, and bulkheads in submarines and airplanes.

In general, the plate problem has been the subject of intensive investigations. The solution to the plate equations are found in several manners. For some cases, an "exact" solution can be obtained if the boundary conditions of the plate are known. If the plate has unusual boundaries, then approximate techniques must be employed.

They are usually subdivided into the following principle categories based on their structural action [1]:

1. Stiff Plates: Thin plates with flexural rigidity, carrying loads two-dimensionally, mostly by internal (bending and torsional) moments and by transverse shears, generally in a manner similar to beams.

2. Membranes: Thin plates without flexural rigidity, carry the lateral loads by axial and central (in the plane of the plate) shear forces. This load-carrying action can be approximated by a network of stressed cables since, because of their extreme thinness; their moment resistance may be neglected.

3. Flexible Plates: A combination of stiff plates and membranes which carry external loads by the combined action of internal moments, transverse and central shear forces, and axial forces.

4. Thick Plates: Internal stress condition resembles that of three dimensional continua.

Plate theories are grouped according to their stress-strain relationships. The "linear elastic" plate theories are based on the assumption of a linear relationship between stress and strain in the form of a well known Hooke's law, whereas nonlinear elasticity and plasticity consider more complex stress-strain relationships. These theories distinguish sharply between structures having small deflections and those having large deflections. For small deflections, the law of superposition is generally applicable, while for the large deflections, second order theories must be used [1].

1.2 Literature Survey

The analysis of plates first started in the 1800's. Euler solved free vibrations of a flat plate using a mathematical approach for the first time. German physicist Chladni discovered the various modes of free vibrations of plates. Then later on, the theory of elasticity was formulated. Navier can be considered as the originator of the modern theory of elasticity. Navier's numerous scientific activities included the solution of various plate problems. He also derived the exact differential equation for rectangular plates with flexural resistance. For the solution to certain boundary value problems, Navier introduced exact methods which transformed differential equations to algebraic equations. Poisson extended the use of governing plate equation to lateral vibration of circular plates. Later, the theory of elasticity was extended as

there were many researchers working on the plate and the extended plate theory was formulated. Kirchhoff is considered as the one who formulated the extended plate theory [2-5].

In the late 1900's, the theory of finite elements method was evolved, which can be considered as a basis for the analysis on complex structures. However the analysis using finite elements are now being carried out using comprehensive software packages which require high CPU resources to compute the results. Another method for analysis of plates statically and dynamically was later developed for arbitrary shapes using advanced finite elements. In addition to these, a method called the weighted residual method which was used in analysis of plates even before the finite element method of analyzing the plate was developed.

The stress analysis of circular plates attracts the attention of the researchers as a basic mechanical problem. The formulations of the stresses and displacements for such elements under different conditions are given in many text books [7-10]. Besides these, studies on the elastic and elastic-plastic analysis of circular plates are performed by many researchers. In addition, homogenous or functionally graded one layer plates, sandwich plates and multi-layer circular plates are studied in the past.

Focusing only on the stress and displacement distributions in one layer circular plate under uniform load, the analytical solution developed by Ding Hao et al. [11] explains rigorously two type of clamped end circular plate behaviour, using a stress function which given by Timoshenko and Goodier [7].

General formula for the stress and displacements in layered elastic system was discussed by Wang Kai [12]. He employed two types of unidirectional (horizontal or vertical) loads and centripetal (horizontal or rotational loads) loading using three types of binding interface conditions: Smooth, continuous interface and semi-bind interface.

The problem of bending of circular plate of variable thickness was first investigated by Hozler [13], while the solution for rectangular plates with variable thickness in one or both direction was attempted first by Olsson [14]. Differential equation of

equilibrium had been obtained for the bending of a normally loaded and uniformly compressed circular plate with a central hole and variable thickness by Chakravorty [15].

Lo et al. [16] concentrated on the solution of the deflection of circular plates of variable thickness that are acted upon by transverse loading. The plates were assumed to be thin plates and the deflections and rotations were assumed to be small. The solution is given in the form of an equivalent system of flat plates that replaces the original variable thickness plate. Due to the linearity of the governing equation, the sum of the deflections, bending moments and bending stresses of the flat plates by the equivalent system is equal to that of the corresponding elements of the original variable thickness plate.

A limit analysis are utilized for a circular plate by Ghorashi et al. [17], by taking both thickness and the imposed load arbitrary functions of the plate radial coordinate, then finding the maximum load by using square and Tresca yield criterion for simply supported edge circular plate.

A new class of materials known as "functionally graded materials" (FGM) has been introduced in which the material properties vary continuously in one or more directions according to a specific profile. These materials are microscopically heterogeneous and are typically made of isotropic components such as metals and ceramics. FGMs exploit the ideal performance of their composition, e.g. heat and corrosion resistance of ceramics on one side, and mechanical strength and toughness of metals on the other side of a body [18].

The concept of functionally graded materials was initially proposed in 1984 by a group of scientists in Sendai, Japan (Yamanouchi et al.[19]; Koizumi, [20]). Since then, FGMs have been of intensive research interests. Due to the continuously varying material properties in space on the macroscopic scale, FGMs are usually superior to the conventional fiber-matrix materials in mechanical behavior, especially under thermal loads. Because of no internal seams or boundaries, stress

peaks are missing in FGM structures when external loadings are applied, and failure from interfacial debonding and stress concentration can be avoided.

Investigation of isotropic functionally graded circular plate subjected to transverse varying load qrk was done by Li et al. [21], by using a stress function. In a research performed by Lei et al. [22], in which the displacment function of a functionally graded circular plate is expanded to Fourier - Bessel series based on the basic equations of equilibrium of isotropic material, they obtained general equation for normal and shear stresses by supposing that the poisson's ratio (ν) is constant while Young's modulus (E) depends on z coordinate only. A general formulation for functionally graded circular three layered (sandwich) plates by using sinusoidal shear deformation plate theory (SSDPT) was obtained by Zenkour [23]. He investigated the deflection and stresses by using sinusoidal shear deformation theory and compared the results with first order deformation plate theory (FSDPT), third order deformation plate theory (TSDPT) and classical plate theory (CLPT) .

First order deformation plate theory (FSDPT) (Mindlin theory) was used by Reddy et al. [24] to obtain the solution of deflection and axisymmetric bending of functionally graded circular and annular plates. Force and moment resultants of the first order plate theory are presented in terms of the corresponding quantities of isotropic plates based on the classical Kirchhoff plate theory. In a comparative study done by Mihai et al. [25], the governing equation for the bending of isotropic plates with clamped and simply support ends were studied by using several known plate theories like first order shear deformation theory, which take in consideration the transverse shear strain, and compare it with classical plate theory (Kirchoff). In addition to these comparisons, he linked the two theories and made two and three dimensional models with ANSYS and SAP 2000 software packages and made comparisons between them.

1.3 Definition of the Problem

The circular plate subjected to a uniform transverse load is one of the classical problems of the elasticity. There are several solutions to this problem. One of the

solutions is the three dimensional solution based on the theory of elasticity. Using the stress-strain relations, strain-displacement relations and equations of equilibrium, the solution of the problem can be obtained. Most of the three dimensional solutions are based on stress functions. In this study, two different three dimensional solutions based on stress functions are handled: The three dimensional solution presented by Barber [26] and the solution presented by Timoshenko and Goodier [7]. Starting from the beginning, these solutions are derived using MATHEMATICA [6] software.

The results obtained for different plate thickness values by these two solutions are then compared with the classical one dimensional solution given by Timoshenko [8], which can be found in most of the elasticity books. In addition, these analytical solutions are compared with a numerical solution based on finite element method. The numerical solution is obtained by using SAP 2000 [27] software, in which shell elements are used.

An isotropic simply supported circular plate with constant thickness (h) and radius (a) which is subjected to transverse uniform load (p) is illustrated in Fig.1.1. The curvilinear coordinate system, with r, θ and z directions, is used in this study.

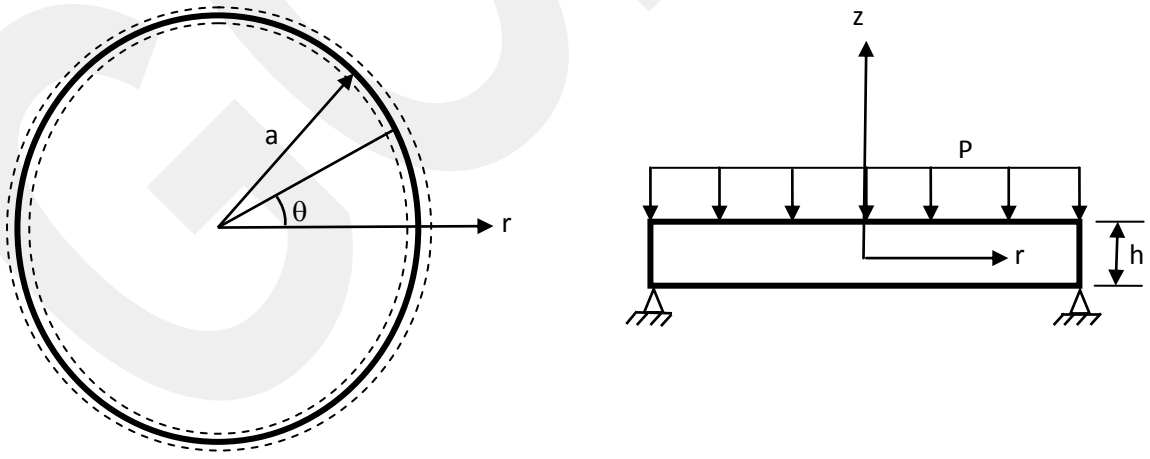

Top view Side view

Fig.1.1 Geometry of a simply supported uniformly loaded circular plate

The general equations of stresses, strains and displacements are derived for uniformly loaded simply supported homogenous circular plate by using the three analytical approaches stated above. In three dimensional solutions, the transverse shear deformation is taken into account, while in one dimensional solution the effects of the transverse shear are neglected. Using these solutions, the stresses, strains and displacements are obtained for different plate thicknesses. In addition to these, in SAP 2000 [27] software, the thin and thick plate assumptions are used in modelling circular plates. The distribution of displacements for different plate thicknesses is obtained numerically using this program.

Finally, the relative errors between the three dimensional and one dimensional solutions and between the three dimensional solutions and SAP 2000 thin and thick models are presented.

1.4 Organization of the Thesis

The definition of the problem, past studies and thesis organization is given in Chapter I. In Chapter II, the analytical expressions for the stresses, strains and displacements are derived by using the three dimensional approach presented by Barber [26] first. Then, the three dimensional solution obtained by using the method presented by Timoshenko and Goodier [7] is given. Finally, the one dimensional solution given by Timoshenko and Woinowsky [8] is presented in this chapter.

The results obtained from the solutions presented in Chapter II are given in Chapter III. In addition, the comparison between SAP 2000 and the analytical solutions are given in this chapter. Finally, the summary and conclusions are given in Chapter IV.

CHAPTER II

FORMULATION AND SOLUTIONS

Cylindrical polar coordinates (r, θ, z) are used in all derivations. It is assumed that the edge of the circular plate is simply supported. First, the governing equations and boundary conditions for a homogenous simply supported circular plate under uniform loading are presented. Then, the two three dimensional solutions, in which stress functions are used, are introduced. Finally, the one dimensional solution for the problem is presented.

All derivations are made by MATHEMATICA [6] program and for each solution, the stresses, displacements and strains are obtained using this software. In the derivations, the radius of the plate is defined as (a) and the thickness of it is taken as (h).

2.1 Governing equations

The equilibrium equations for the uniformly loaded circular plate in transverse direction are given as:

$$\frac{\partial \sigma_r}{\partial r} + \frac{\partial \tau_{rz}}{\partial z} + \frac{\sigma_r - \sigma_\theta}{r} = 0 \qquad (1)$$

$$\frac{\partial \tau_{rz}}{\partial r} + \frac{\partial \sigma_z}{\partial z} + \frac{\tau_{rz}}{r} = 0 \qquad (2)$$

Here σ_r is the radial stress, σ_θ the tangential stress, τ_{rz} the shear stress and σ_z is the transverse stress.

On the other hand, the generalized Hooke's Law gives the following equations:

$$\epsilon_r = \frac{1}{E}\left(\sigma_r - \nu(\sigma_z + \sigma_\theta)\right) \tag{3}$$

$$\epsilon_\theta = \frac{1}{E}\left(\sigma_\theta - \nu(\sigma_r + \sigma_z)\right) \tag{4}$$

$$\epsilon_z = \frac{1}{E}\left(\sigma_z - \nu(\sigma_r + \sigma_\theta)\right) \tag{5}$$

$$\gamma_{rz} = \frac{\partial u}{\partial z} + \frac{\partial w}{\partial r} \tag{6}$$

The strain displacement relations in cylindrical polar coordinates can be written as:

$$\epsilon_r = \frac{\partial u}{\partial r} \tag{7}$$

$$\epsilon_\theta = \frac{u}{r} \tag{8}$$

$$\epsilon_z = \frac{\partial w}{\partial z} \tag{9}$$

The boundary conditions at the upper and lower faces of the uniformly loaded simply supported circular plate are

$$\sigma_z = -p \ , \ \tau_{rz} = 0 \quad \text{at } z = \frac{h}{2} \qquad \text{(upper face)} \tag{10}$$

$$\sigma_z = 0 \ , \ \tau_{rz} = 0 \quad \text{at } z = -\frac{h}{2} \qquad \text{(bottom face)} \tag{11}$$

It should be noted that (p) is the uniform loading at the upper face of the plate. At the bottom face of the plate the shear stress and transverse stress is zero.

In addition, the boundary conditions at the edge of the circular plate are:

$$\int_{-h/2}^{h/2} z\ \sigma_r dz = 0 \qquad r = a \tag{12}$$

$$\int_{-h/2}^{h/2} \sigma_r dz = 0 \qquad r = a \tag{13}$$

In Eq. (12), the integral gives the total moment at the edge and in Eq. (13) it gives the total horizontal force at the edge. These two equations states that moment M=0 and horizontal force N=0 at r=a.

Finally, the transverse displacement at the edge is given as

$$w = 0 \qquad \text{at } r = a, \qquad z = 0 \tag{14}$$

2.2 Three Dimensional Solutions

2.2.1 Barber's Three Dimensional Solution

Many problems in stress analysis, which are of practical importance, are concerned with a solid of revolution deformed symmetrically with respect of axis of symmetry of revolution. The deformation being symmetrical with respect to z-axis, it follows that the stress components are independent of the angle θ, and all the derivatives with respect to θ will vanish. The components of shearing stresses $\tau_{r\theta}$ and τ_{rz} will also vanish due to symmetry [26].

A fifth order potential function ϕ with 4 constants (A5, A4, A3, A2) and a fourth order potential function ω with 4 constants (B4, B3, B2, B1) are considered in the solution of the problem. They are

$$\phi = \frac{A5}{8}(8z^5 - 40z^3r^2 + 15zr^4) + \frac{A4}{8}(8z^4 - 24z^2r^2 + 3r^4) + \frac{A3}{2}(2z^3 - 3zr^2) + \frac{A2}{2}(2z^2 - r^2) \quad (15)$$

$$\omega = \frac{B4}{8}(8z^4 - 24z^2r^2 + 3r^4) + \frac{B3}{2}(2z^3 - 3zr^2) + \frac{B2}{2}(2z^2 - r^2) + B1z \quad (16)$$

The following stress expressions in terms of the two stress function, which are given by Green and Zerna's in Barber [26] are used in the derivations:

$$\sigma_r = \frac{\partial^2\phi}{\partial r^2} + z\frac{\partial^2\omega}{\partial r^2} - 2\nu\frac{\partial\omega}{\partial z} \quad (17)$$

$$\sigma_\theta = \frac{1}{r}\frac{\partial\phi}{\partial r} + \frac{1}{r^2}\frac{\partial^2\phi}{\partial\theta^2} + \frac{z}{r}\frac{\partial\omega}{\partial r} + \frac{z}{r^2}\frac{\partial^2\omega}{\partial\theta^2} - 2\nu\frac{\partial\omega}{\partial z} \quad (18)$$

$$\sigma_z = \frac{\partial^2\phi}{\partial^2 z} + z\frac{\partial^2\omega}{\partial^2 z} - 2(1-\nu)\frac{\partial\omega}{\partial z} \quad (19)$$

$$\tau_{rz} = \frac{\partial^2\phi}{\partial r\,\partial z} + z\frac{\partial^2\omega}{\partial r\,\partial z} - (1-2\nu)\frac{\partial\omega}{\partial r} \quad (20)$$

$$\tau_{r\theta} = \frac{1}{r}\frac{\partial^2\phi}{\partial r\,\partial\theta} - \frac{1}{r^2}\frac{\partial\phi}{\partial\theta} + \frac{z}{r}\frac{\partial^2\omega}{\partial r\,\partial\theta} - \frac{z}{r^2}\frac{\partial\omega}{\partial\theta} \quad (21)$$

$$\tau_{\theta z} = \frac{1}{r}\frac{\partial^2\phi}{\partial z\,\partial\theta} + \frac{z}{r}\frac{\partial^2\omega}{\partial z\,\partial\theta} - \frac{1-2\nu}{r}\frac{\partial\omega}{\partial\theta} \quad (22)$$

Since the problem is axisymmetric, the transverse shear stresses in Eqs. 21 and 22 vanish and are not considered in the derivations ($\tau_{r\theta} = \tau_{\theta z} = 0$). The stresses can be

obtained by substituting the two potential functions given in Eqs. (15) and (16) into Eqs. (17) - (20). They become

$$\sigma_r = -A2 - 3A3z + \frac{1}{8}A4(36r^2 - 48z^2) + \frac{1}{8}A5(180r^2z - 80z^3) - 2B1\nu + B2(-z - 4z\nu) + B3(-3z^2 + (3r^2 - 6z^2)\nu) + B4\left(\frac{1}{8}z(36r^2 - 48z^2) + \frac{1}{4}(48r^2z - 32z^3)\nu\right) \quad (23)$$

$$\sigma_\theta = -A2 - 3A3z + \frac{3}{2}A4(r^2 - 4z^2) + \frac{1}{2}A5(15r^2z - 20z^3) - 2B1\nu + \frac{1}{2}B2(-2z - 8z\nu) + \frac{1}{2}B3(-6z^2 + 6r^2\nu - 12z^2\nu) + \frac{1}{2}B4(3r^2z - 12z^3 + 24r^2z\nu - 16z^3\nu) \quad (24)$$

$$\sigma_z = 2A2 + 6A3z + \frac{1}{8}A4(-48r^2 + 96z^2) + \frac{1}{8}A5(-240r^2z + 160z^3) + B2\big(2z - 4z(1-\nu)\big) + B3\big(6z^2 + (3r^2 - 6z^2)(1-\nu)\big) + B4\left(\frac{1}{8}z(-48r^2 + 96z^2) + \frac{1}{4}(48r^2z - 32z^3)(1-\nu)\right) - 2B1(1-\nu) \quad (25)$$

$$\tau_{rz} = -3A3r - 12A4rz + \frac{15}{2}A5r(r^2 - 4z^2) + \frac{1}{2}B2r(2 - 4\nu) - 6B3rz\nu - \frac{3}{2}B4r\big(r^2(1-2\nu) + 4z^2(1+2\nu)\big) \quad (26)$$

It should be noted that σ_z is an even function in r and τ_{rz} is an odd function in r. Due to this reason, the boundary conditions given in Eqs. (10) and (11) require us to equate coefficients of r^2 and r^0 in σ_z and of r^3 and r in τ_{rz} on each of the boundaries z=h/2 and z=-h/2. This leads the following equations:

$$\frac{15A5}{2} - \frac{3}{2}B4(1-2\nu) = 0 \quad (27)$$

$$-3A3 - 6A4h - \frac{15A5h^2}{2} + \frac{1}{2}B2(2 - 4\nu) - 3B3h\nu - \frac{3}{2}B4h^2(1 + 2\nu) = 0 \qquad (28)$$

$$-3A3 + 6A4h - \frac{15A5h^2}{2} + \frac{1}{2}B2(2 - 4\nu) + 3B3h\nu - \frac{3}{2}B4h^2(1 + 2\nu) = 0 \qquad (29)$$

$$2A2 - 3A3h + 3A4h^2 + \frac{3B3h^2}{2} - \frac{5A5h^3}{2} - \frac{3B4h^3}{2} + B2\big(-h + 2h(1 - \nu)\big)$$
$$+ r^2\big(-6A4 + 15A5h + 3B4h + 3B3(1 - \nu) - 6B4h(1 - \nu)\big) - 2B1(1 - \nu)$$
$$-\frac{3}{2}B3h^2(1 - \nu) + B4h^3(1 - \nu) = 0 \qquad (30)$$

$$2A2 + 3A3h + 3A4h^2 + \frac{3B3h^2}{2} + \frac{5A5h^3}{2} + \frac{3B4h^3}{2} + B2\big(h - 2h(1 - \nu)\big)$$
$$+ r^2\big(-6A4 - 15A5h - 3B4h + 3B3(1 - \nu) + 6B4h(1 - \nu)\big) - 2B1(1 - \nu)$$
$$-\frac{3}{2}B3h^2(1 - \nu) - B4h^3(1 - \nu) = -q \qquad (31)$$

$$-6A4 - 15A5h - 3B4h + 3B3(1 - \nu) + 6B4h(1 - \nu) = 0 \qquad (32)$$

$$-6A4 + 15A5h + 3B4h + 3B3(1 - \nu) - 6B4h(1 - \nu) = 0 \qquad (33)$$

Two additional equations are introduced by substituting the radial stress (23) into the boundary conditions (12) and (13). Evaluating the two integrals give:

$$-A2h + \frac{9}{2}a^2A4h - \frac{A4h^3}{2} - \frac{B3h^3}{4} - 2B1h\nu + 3a^2B3h\nu - \frac{1}{2}B3h^3\nu = 0 \qquad (34)$$

$$-\frac{A3h^3}{4} + \frac{15}{8}a^2A5h^3 - \frac{B2h^3}{12} + \frac{3}{8}a^2B4h^3 - \frac{A5h^5}{8} - \frac{3B4h^5}{40} - \frac{1}{3}B2h^3\nu + a^2B4h^3\nu$$
$$-\frac{1}{10}B4h^5\nu = 0 \qquad (35)$$

Solving these equations (Eqs.(27)-(35)) with MATHEMATICA for the constants A2, A3, A4, A5, B1, B2, B3 and B4 gives:

$$A2 = -\frac{p\nu}{2(1+\nu)} \tag{36}$$

$$A3 = -\frac{p(5a^2(3+\nu)(-1+2\nu)+h^2(7+(17-2\nu)\nu))}{40h^3(1+\nu)} \tag{37}$$

$$A4 = 0 \tag{38}$$

$$A5 = \frac{p-2p\nu}{20h^3} \tag{39}$$

$$B1 = \frac{p}{4+4\nu} \tag{40}$$

$$B2 = \frac{3p(-h^2(-3+\nu)+5a^2(3+\nu))}{40h^3(1+\nu)} \tag{41}$$

$$B3 = 0 \tag{42}$$

$$B4 = \frac{p}{4h^3} \tag{43}$$

After substituting the above 8 constants into stress expressions (Eqs. (23) –(26)) the stress fields are obtained as:

$$\sigma_r = -\frac{pz^3(2+\nu)}{h^3} - \frac{3p(a-r)(a+r)z(3+\nu)}{4h^3} + \frac{3pz}{10h} + \frac{3pz\nu}{20h} \tag{44}$$

$$\sigma_\theta = -\frac{pz^3(2+\nu)}{h^3} + \frac{3pz(-a^2(3+\nu)+r^2(1+3\nu))}{4h^3} + \frac{3pz}{10h} + \frac{3pz\nu}{20h} \tag{45}$$

$$\sigma_z = -\frac{p(h-z)(h+2z)^2}{2h^3} \tag{46}$$

$$\tau_{rz} = \frac{3pr(h^2-4z^2)}{4h^3} \tag{47}$$

From the generalized Hook's law, the strains given in Eqs. (3), (4), (5) and (6) can be determined by substitution of the final stress terms. They are:

$$\epsilon_r = -\frac{3pz(-9+\nu)\nu}{20Eh} + \frac{p(h^3+3a^2z)\nu}{2Eh^3} + \frac{pz^3(-2+\nu)(1+\nu)}{Eh^3} + \frac{3pz(a^2(-3+\nu^2)-3r^2(-1+\nu^2))}{4Eh^3} + \frac{3pz}{10hE} \tag{48}$$

$$\epsilon_\theta = -\frac{3pz(-9+\nu)\nu}{20Eh} + \frac{pz(3a^2\nu+2z^2(-2+\nu)(1+\nu))}{2Eh^3} + \frac{3pz(a^2(-3+\nu^2)-r^2(-1+\nu^2))}{4Eh^3} + \frac{3pz}{10hE} + \frac{p\nu}{2E} \tag{49}$$

$$\epsilon_z = -\frac{p(h+3z)}{2Eh} - \frac{3pz\nu(2+\nu)}{10Eh} + \frac{pz(4z^2(1+\nu)^2+3\nu(-2r^2(1+\nu)+a^2(3+\nu)))}{2Eh^3} \tag{50}$$

$$\gamma_{rz} = \frac{\tau_{rz}}{G} = \frac{3\,p\,r\,(h^2-4z^2)}{4\,G\,h^3} \tag{51}$$

Using the relation between the radial strain and the radial displacement in Eq. (7), the radial displacement can be found as:

$$u = \frac{prz^3(-2+\nu)(1+\nu)}{Eh^3} - \frac{3prz(-2+(-9+\nu)\nu)}{20Eh}$$
$$+ \frac{3prz(a^2(-3+\nu^2) - r^2(-1+\nu^2))}{4Eh^3} + \frac{pr(h^3+3a^2z)\nu}{2Eh^3} \quad (52)$$

Using Eq.(6), the derivative of deflection w can be written as:

$$\frac{\partial w}{\partial r} = \gamma_{rz} - \frac{\partial u}{\partial z} = -\frac{3Pr(3+\nu)a^2(-1+\nu)}{8Gh^3(1+\nu)}$$
$$+ \frac{3Pr(h^2(8+\nu+\nu^2)+5(1+\nu)(-4z^2\nu+r^2(-1+\nu)))}{40Gh^3(1+\nu)} \quad (53)$$

The first term (shear strain γ_{rz}) in the above equation is given in Eq. (51), and the second term is the derivative of radial displacement according to the (z). Solving the above equation, which is a first order differential equation, to determine the deflection (w) at the neutral axis of the plate (z=0) by using the boundary conditions (as the deflection at the edge is equal to zero (w (a) = 0)) gives:

$$w(r,0) = \frac{3(a+r)(5+\nu)a^2(-1+\nu)P(a-r)}{32Gh^3(1+\nu)}$$
$$- \frac{3(a+r)P(a-r)(2h^2(8+\nu+\nu^2)+5r^2(-1+\nu^2))}{160Gh^3(1+\nu)} \quad (54)$$

It should be noted that the stress expressions obtained in this solution satisfies the two equilibrium equations given in Eqs. (1) and (2).

2.2.2 Solution Obtained by Timoshenko et al. [7]

The stress function solution obtained by Timoshenko et al. [7] for the uniformly loaded clamped end circular plates are adopted for simply supported circular plates under uniform loading.

The equations of equilibrium given in Eqs. (1) and (2), and strain displacement relations given in Eqs. (6) to (9) are also used in this solution. In terms of the stress function, the stress and displacement expressions can be written as [7]:

$$\sigma_r = \frac{\partial}{\partial z}\left(\nu\nabla^2\phi - \frac{\partial^2\phi}{\partial r^2}\right) \tag{55}$$

$$\sigma_\theta = \frac{\partial}{\partial z}\left(\nu\nabla^2\phi - \frac{1}{r}\frac{\partial\phi}{\partial r}\right) \tag{56}$$

$$\sigma_z = \frac{\partial}{\partial z}((2-\nu)\nabla^2\phi - \frac{\partial^2\phi}{\partial z^2}) \tag{57}$$

$$\tau_{rz} = \frac{\partial}{\partial r}((1-\nu)\nabla^2\phi - \frac{\partial^2\phi}{\partial z^2}) \tag{58}$$

$$u = -\frac{1}{2G}\frac{\partial^2\phi}{\partial z\,\partial r} \tag{59}$$

$$w = \frac{1}{2G}(\,2(1-\nu)\nabla^2\phi - \frac{\partial^2\phi}{\partial z^2}) \tag{60}$$

It should be noted that the stress function ϕ should satisfy the biharmonic equation

$$\nabla^2\nabla^2\phi = 0 \tag{61}$$

which is

$$\left(\frac{\partial^2}{\partial r^2} + \frac{1}{r}\frac{\partial}{\partial r} + \frac{1}{r^2}\frac{\partial^2}{\partial\theta^2} + \frac{\partial^2}{\partial z^2}\right)\left(\frac{\partial^2}{\partial r^2} + \frac{1}{r}\frac{\partial}{\partial r} + \frac{1}{r^2}\frac{\partial^2}{\partial\theta^2} + \frac{\partial^2}{\partial z^2}\right) = 0 \tag{62}$$

Due to axisymmetry, the biharmonic equation is independent of θ and it reduces to

$$\left(\frac{\partial^2}{\partial r^2} + \frac{1}{r}\frac{\partial}{\partial r} + \frac{\partial^2}{\partial z^2}\right)\left(\frac{\partial^2}{\partial r^2} + \frac{1}{r}\frac{\partial}{\partial r} + \frac{\partial^2}{\partial z^2}\right) = 0 \tag{63}$$

The streses represented by the stress function should also satisfy the equations of equilibrium given in Eqs. (1) and (2). The boundary conditions for the problem are given in Eqs.(10), (11), (12) and (13).

The stress function ϕ, which should satisfy the biharmonic equation is derived from Legendre polynomials after solving a second order partial differential equation. Introducing the relation between R, z and r in polar coordinates (as shown in Fig. 2.1), the following expressions can be obtained:

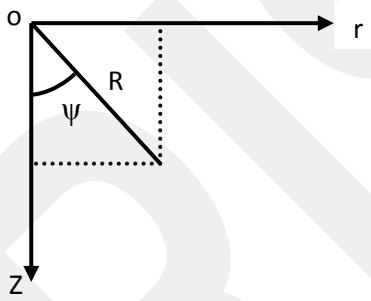

Fig.2.1 Polar coordinates

$$\cos(\psi) = \mathrm{x} = \frac{\mathrm{z}}{\mathrm{R}} \quad ; \quad \mathrm{x} = \frac{\mathrm{z}}{\sqrt{\mathrm{r}^2 + \mathrm{z}^2}} \tag{64}$$

In addition, the following relations are valid:

$$\frac{\partial^2}{\partial \mathrm{r}^2} + \frac{\partial^2}{\partial \mathrm{z}^2} = \frac{\partial^2}{\partial \mathrm{R}^2} + \frac{1}{\mathrm{R}} * \frac{\partial}{\partial \mathrm{R}} \mathrm{ctn}(\psi) \frac{\partial}{\partial \psi} + \frac{1}{\mathrm{R}^2} * \frac{\partial^2}{\partial \psi^2} \tag{65}$$

$$\frac{1}{\mathrm{r}} * \frac{\partial}{\partial \mathrm{r}} = \frac{1}{\mathrm{R}} * \frac{\partial}{\partial \mathrm{R}} + \frac{\mathrm{ctn}(\psi)}{\mathrm{R}^2} \frac{\partial}{\partial \psi} \tag{66}$$

In polar coordinates, the biharmonic equation can be written as

$$\left(\frac{\partial^2}{\partial R^2}+\frac{2}{R}*\frac{\partial}{\partial R}+\frac{1}{R^2}\operatorname{ctn}(\psi)\frac{\partial}{\partial \psi}+\frac{1}{R^2}*\frac{\partial^2}{\partial \psi^2}\right)\left(\frac{\partial^2 \phi}{\partial R^2}+\frac{2}{R}*\frac{\partial \phi}{\partial R}+\frac{1}{R^2}\operatorname{ctn}(\psi)\frac{\partial \phi}{\partial \psi}+\frac{1}{R^2}*\frac{\partial^2 \phi}{\partial \psi^2}\right)=0 \quad (67)$$

The expression in the first parenthesis can be defined as A and the expression in the second parenthesis can be defined as B. They are:

$$A=\left(\frac{\partial^2}{\partial R^2}+\frac{2}{R}*\frac{\partial}{\partial R}+\frac{1}{R^2}\operatorname{ctn}(\psi)\frac{\partial}{\partial \psi}+\frac{1}{R^2}*\frac{\partial^2}{\partial \psi^2}\right) \quad (68)$$

$$B=\left(\frac{\partial^2 \phi}{\partial R^2}+\frac{2}{R}*\frac{\partial \phi}{\partial R}+\frac{1}{R^2}\operatorname{ctn}(\psi)\frac{\partial \phi}{\partial \psi}+\frac{1}{R^2}*\frac{\partial^2 \phi}{\partial \psi^2}\right) \quad (69)$$

It should be noted that the solution of B is also the solution of $\nabla^2\nabla^2\phi=0$. Therefore the differential equation which is to be solved is

$$\left(\frac{\partial^2 \phi}{\partial R^2}+\frac{2}{R}*\frac{\partial \phi}{\partial R}+\frac{1}{R^2}\operatorname{ctn}(\psi)\frac{\partial \phi}{\partial \psi}+\frac{1}{R^2}*\frac{\partial^2 \phi}{\partial \psi^2}\right)=0 \quad (70)$$

Solution of the above equations is in the form of $\phi_n = R^n * \psi_n$. Here ψ_n is function of angle ψ as shown in Fig. 2.1. Inserting ϕ_n into (B) results in.

$$\frac{1}{\sin(\psi)}\frac{d}{d\psi}\left(\sin(\psi)\frac{d\psi_n}{d\psi}\right)+n(n+1)\psi_n=0 \quad (71)$$

Taking $x=\cos(\psi)$, the equation becomes

$$(1-x^2)\frac{d^2\psi_n}{dx^2}-2x\frac{d\psi_n}{dx}+n(n+1)\psi_n=0 \quad (72)$$

This equation is the Legendre equation, which has two basic solutions $P_n(x)$ and $Q_n(x)$. $P_n(x)$ represent the Legendre function of the first kind and $Q_n(x)$ represents Legendre function of the second kind. The general solution of Eq. (72) is

$$\psi_n = C_1 P_n(x) + C_2 Q_n(x) \tag{73}$$

The Legendre polynomials for n=0 to 6 are

$$n=0 \qquad p_0(x) = 1 \tag{74}$$

$$n=1 \qquad p_1(x) = x \tag{75}$$

$$n = 2 \quad p_2(x) = \frac{1}{2}(-1 + 3x^2) \tag{76}$$

$$n = 3 \quad p_3(x) = \frac{1}{2}(-3x + 5x^3) \tag{77}$$

$$n = 4 \quad p_4(x) = \frac{1}{8}(3 - 30x^2 + 35x^4) \tag{78}$$

$$n = 5 \quad p_5(x) = \frac{1}{8}(15x - 70x^3 + 63x^5) \tag{79}$$

$$n = 6 \quad p_6(x) = \frac{1}{16}(-5 + 105x^2 - 315x^4 + 231x^6) \tag{80}$$

Restoring r and z by means of Eq. (64) and considering

$$\phi_n = R^n * \psi_n \tag{81}$$

the following expressions can be obtained:

$$\phi_0 = A_0 R^0 \psi_0 = A_0 * 1 * 1 = A_0 \tag{82}$$

$$\phi_1 = A_1 R^1 \psi_1 = A_1 \sqrt{r^2 + z^2}.\frac{z}{\sqrt{r^2 + z^2}} = A_1 z \tag{83}$$

$$\phi_2 = A_2 R^2 \psi_2 = A_2 * \sqrt{r^2 + z^2} * \frac{1}{2}\left(3\left(\frac{z}{\sqrt{r^2 + z^2}}\right)^2 - 1\right)$$

$$= A_2 * (r^2 + z^2).\left(\frac{3}{2}\frac{z^2}{(r^2 + z^2)} - \frac{1}{2}\right) = \frac{3A_2}{2}z^2 - \frac{A_2(r^2 + z^2)}{2}$$

$$= A_2\left(z^2 - \frac{(r^2 + z^2)}{3}\right) \tag{84}$$

$$\phi_3 = A_3 R^3 \psi_3 = A_3 (r^2 + z^2)^{3/2} * \frac{1}{2}\left(-3\frac{z}{\sqrt{r^2 + z^2}} + 5\frac{z^3}{\left(\sqrt{r^2 + z^2}\right)^{3/2}}\right)$$

$$= A_3\left(5z^3 - z(r^2 + z^2)\right) = A_3\left(z^3 - \frac{3z(r^2 + z^2)}{5}\right) \tag{85}$$

$$\phi_4 = A_3 R^4 \psi_4 = A_4 (r^2 + z^2)^2 * \frac{1}{8}(3 - 30\frac{z^2}{r^2 + z^2} + 35\frac{z^4}{(r^2 + z^2)^2})$$

$$= A_4(35z^4 - 30z^2(r^2 + z^2) + 3(r^2 + z^2)^2$$

$$= A_4(z^4 - \frac{30}{35}z^2(r^2 + z^2) + \frac{3}{35}(r^2 + z^2)^2)$$

$$= A_4\left(z^4 - \frac{6}{7}z^2(r^2 + z^2) + \frac{3}{35}(r^2 + z^2)^2\right) \tag{86}$$

$$\phi_5 = A_5 R^5 \psi_5 = A_5 (r^2 + z^2)^{\frac{5}{2}} * \frac{1}{8}\left(\frac{15\,z}{(r^2 + z^2)^{\frac{1}{2}}} - \frac{70\,z^3}{(r^2 + z^2)^{\frac{3}{2}}} + \frac{63\,z^5}{(r^2 + z^2)^{\frac{5}{2}}}\right)$$

$$= A_5(63z^5 - 70z^3(r^2 + z^2) + 15z(r^2 + z^2)^2)$$

$$= A_5\left(z^5 - \frac{70}{63}z^3(r^2 + z^2) + \frac{15}{63}z(r^2 + z^2)^2\right)$$

$$= A_5\left(z^5 - \frac{10}{9}z^3(r^2 + z^2) + \frac{5}{21}z(r^2 + z^2)^2\right) \tag{87}$$

$$\phi_6 = A_6\left(z^6 - \frac{15}{11}z^4(r^2 + z^2) + \frac{5}{11}z^2(r^2 + z^2)^2 - \frac{5}{231}(r^2 + z^2)^3\right) \tag{88}$$

If $R^n * \psi_n$ is solution of B, then $R^{n+2} * \psi_n$ is a solution of A*B. Therefore, a new set of potential functions can be obtained as,

$$\bar{\phi}_2 = B_2 R^2 \psi_0 = B_2 * \left(\sqrt{r^2 + z^2}\right)^2 \; A_0 \, B_2 = B_2 \left(r^2 + z^2\right) \tag{89}$$

$$\bar{\phi}_3 = B_3 R^2 \psi_1 = B_2 * \left(\sqrt{r^2 + z^2}\right)^2 A_1 \, z \, B_3 = B_3 \, z \left(r^2 + z^2\right) \tag{90}$$

$$\bar{\phi}_4 = B_4 \, R^2 \, \psi_2 = \left(r^2 + z^2\right) \; A_2 \left(z^2 - \frac{\left(r^2 + z^2\right)}{3}\right) B_4$$

$$= \left(r^2 + z^2\right) A_2 \, \frac{\left(3z^2 - r^2 - z^2\right)}{3} B_4 = \; B_4 \left(r^2 + z^2\right) \left(2z^2 - r^2\right) \tag{91}$$

$$\bar{\phi}_5 = B_5 \, R^2 \, \psi_3 = \left(r^2 + z^2\right) \; A_3 \left(z^3 - \frac{3z\left(r^2 + z^2\right)}{5}\right) B_5$$

$$= \left(r^2 + z^2\right) A_3 \, \frac{\left(5z^3 - 3zr^2 - 3z^3\right)}{5} \, B_5 = \; B_5 \left(r^2 + z^2\right) \left(2z^3 - 3zr^2\right) \tag{92}$$

$$\bar{\phi}_6 = B_6 \, R^2 \, \psi_4 = \left(r^2 + z^2\right) A_4 \left(z^4 - \frac{6}{7} z^2 \left(r^2 + z^2\right) + \frac{3}{35} \left(r^2 + z^2\right)^2\right) B_6$$

$$= B_6 \left(8z^4 - 24z^2 r^2 + 3r^4\right) \left(r^2 + z^2\right) = \; B_6 \left(8z^6 - 16z^4 r^2 - 21z^2 r^4 + 3r^6\right) \tag{93}$$

The sixth order potential stress function is introduced by combining $\phi_6, \bar{\phi}_6, \phi_4, \bar{\phi}_4, \phi_3, \bar{\phi}_3$ and $\phi_2, \bar{\phi}_2$ which are given in Eqs. (84), (85), (86), (88), (89), (90), (91) and (93). It is

$$\phi = A_6(16z^6 - 120z^4 r^2 + 90z^2 r^4 - 5r^6) + B_6(8z^6 - 16z^4 r^2 - 21z^2 r^4 + 3r^6) + A_4(8z^4 - 24r^2 z^2 + 3r^4) + B_4(2z^4 + r^2 z^2 - r^4) + A_3(2z^3 - 3r^2 z) + B_3(z^3 + r^2 z) + A_2(2z^2 - r^2) + B_2(r^2 + z^2) \tag{94}$$

Substituting stress function (94) into stress and displacement equations (55), (56), (57), (58), (59) and (60), the following expressions are obtained:

$$\sigma_r = 6A_3 + 96zA_4 + 240z(-9r^2 + 4z^2)A_6 + 2(-1 + 5\nu)B_3 + 4z(-1 + 14\nu)B_4 + 8z\left(r^2(63 - 132\nu) + 8z^2(2 + 11\nu)\right)B_6 \quad (95)$$

$$\sigma_\theta = 6A_3 + 96zA_4 + 240z(-3r^2 + 4z^2)A_6 + 2(-1 + 5\nu)B_3 + 4z(-1 + 14\nu)B_4 + 8z\left(3r^2(7 - 44\nu) + 8z^2(2 + 11\nu)\right)B_6 \quad (96)$$

$$\sigma_z = -12A_3 - 192zA_4 - 960z(-3r^2 + 2z^2)A_6 + 2(7 - 5\nu)B_3 + 8z(8 - 7\nu)B_4 + 32z\left(2z^2(7 - 11\nu) + r^2(-54 + 33\nu)\right)B_6 \quad (97)$$

$$\tau_{rz} = 96rA_4 - 720r(r^2 - 4z^2)A_6 + 4r(-8 + 7\nu)B_4 + 24r\left(r^2(18 - 11\nu) + 4z^2(-7 + 11\nu)\right)B_6 \quad (98)$$

$$u = \frac{1}{2\,G}(6rA_3 + 96rzA_4 - 240rz(3r^2 - 4z^2)A_6 - 2rB_3 - 4rzB_4 + 8rz(21r^2 + 16z^2)B_6) \quad (99)$$

$$w = \frac{1}{2G}(-4A_2 - 12zA_3 + (48r^2 - 96z^2)A_4 + \left(-180r^4 - 480z^2(-3r^2 + z^2)\right)A_6 - 2(-5 + 6\nu)B_2 - 2z(-7 + 10\nu)B_3 + 2\left(4z^2(4 - 7\nu) + r^2(-15 + 14\nu)\right)B_4 - 2\left(48r^2z^2(9 - 11\nu) + 8z^4(-7 + 22\nu) + r^4(-87 + 66\nu)\right)B_6) \quad (100)$$

The above equation (Eq. (100)) can be simplified by taking $C_2 = -4A_2 - 2(-5 + 6\nu)B_2$. It becomes

$$w = \frac{1}{2G}(C_2 - 12zA_3 + (48r^2 - 96z^2)A_4 + \left(-180r^4 - 480z^2(-3r^2 + z^2)\right)A_6 - 2z(-7 + 10\nu)B_3 + 2\left(4z^2(4 - 7\nu) + r^2(-15 + 14\nu)\right)B_4 - 2\left(48r^2z^2(9 - 11\nu) + 8z^4(-7 + 22\nu) + r^4(-87 + 66\nu)\right)B_6) \quad (101)$$

Using the boundary conditions which are given in Eqs. (12) and (13) and considering Eq. (64), the following relations can be obtained:

$$\int_{-h/2}^{h/2} z\,\sigma_r[a,z]dz = \frac{1}{15}h^3\big(120A_4 + 180(-15a^2+h^2)A_6 + 5(-1+14\nu)B_4 + 6\big(5a^2(21-44\nu)+2h^2(2+11\nu)\big)B_6\big) = 0 \quad (102)$$

$$\int_{-h/2}^{h/2} \sigma_r[a,z]dz = 2h(3A_3 + (-1+5\nu)B_3) = 0 \quad (103)$$

Substituting the deflection at the center (z=0) and edge (r=a) given in Eq. (13) gives:

$$w(a,0) = C_2 + 48a^2A_4 - 180a^4A_6 + 2a^2(-15+14\nu)B_4 - 2a^4(-87+66\nu)B_6 \quad (104)$$

Using the boundary conditions given in Eqs. (10) and (11) and the equations given in Eqs.(102) to (104), the 7 constants are obtained as

$$A_3 = \frac{p(-1+5\nu)}{60(1+\nu)} \quad (105)$$

$$A_4 = \frac{p(5a^2(3+\nu)(-8+7\nu)+h^2(11+(64-7\nu)\nu))}{4480h^3(1+\nu)} \quad (106)$$

$$A_6 = \frac{p(-18+11\nu)}{10560h^3} \quad (107)$$

$$B_3 = -\frac{p}{20(1+\nu)} \quad (108)$$

$$B_4 = -\frac{3p(-h^2(-3+\nu)+5a^2(3+\nu))}{560h^3(1+\nu)} \quad (109)$$

$$B_6 = -\frac{p}{352h^3} \tag{110}$$

$$C_2 = \frac{3a^2p(5a^2(-1+\nu)(5+\nu) - 2h^2(8+\nu+\nu^2))}{80h^3(1+\nu)} \tag{111}$$

After substituting these into the stress and displacement relations the following expressions are obtained:

$$\sigma_r = \frac{pz(3h^2 - 20z^2)(2+\nu)}{20h^3} + \frac{p(-15a^2 + 15r^2)z(3+\nu)}{20h^3} \tag{112}$$

$$\sigma_\theta = \frac{pz(3h^2 - 20z^2)(2+\nu)}{20h^3} + \frac{3pz(-a^2(3+\nu) + r^2(1+3\nu))}{4h^3} \tag{113}$$

$$\sigma_z = -\frac{p(h-z)(h+2z)^2}{2h^3} \tag{114}$$

$$\tau_{rz} = \frac{3pr(h^2 - 4z^2)}{4h^3} \tag{115}$$

$$u = \frac{prz^3(-2+\nu)}{2Gh^3} + \frac{3prz(-1+\nu)(-r^2(1+\nu) + a^2(3+\nu))}{8Gh^3(1+\nu)} + \frac{pr(10h^3\nu - 3h^2z(-2 + (-9+\nu)\nu))}{40Gh^3(1+\nu)} \tag{116}$$

$$w = -\frac{3pz^2\nu(2+\nu)}{40Gh(1+\nu)} + \frac{p(-6a^2h^2 + 6h^2r^2)(8+\nu+\nu^2)}{160Gh^3(1+\nu)} + \frac{p(-40h^3z - 60h^2z^2 - 120r^2z^2\nu(1+\nu) + 40z^4(1+\nu)^2 + 60a^2z^2\nu(3+\nu))}{160Gh^3(1+\nu)} + \frac{p(-1+\nu)(15r^4(1+\nu) - 30a^2r^2(3+\nu) + 15a^4(5+\nu))}{160Gh^3(1+\nu)} \tag{117}$$

By substituting z=0 in the above equation, the deflection of middle surface can be obtained. It's the same as the deflection of the middle surface of Barber's solution which is given in Eq. (54). From the generalized Hook's law, the strains can be determined after substitution of final stress terms as:

$$\epsilon_r = \frac{p(-1+\nu)(-45r^2z(1+\nu)+15a^2z(3+\nu))}{40Gh^3(1+\nu)} + \frac{p(10h^3\nu+20z^3(-2+\nu)(1+\nu)-3h^2z(-2+(-9+\nu)\nu))}{40Gh^3(1+\nu)} \quad (118)$$

$$\epsilon_\theta = \frac{p(-1+\nu)(-15r^2z(1+\nu)+15a^2z(3+\nu))}{40Gh^3(1+\nu)} + \frac{p\left(10h^3\nu+20z^3(-2+\nu)(1+\nu)-3h^2z(-2+(-9+\nu)\nu)\right)}{40Gh^3(1+\nu)} \quad (119)$$

$$\epsilon_z = -\frac{3pr^2z\nu}{2Gh^3} + \frac{pz^3(1+\nu)}{Gh^3} + \frac{p(-40h^3+120a^2z\nu(3+\nu)-24h^2z(5+\nu(2+\nu)))}{160Gh^3(1+\nu)} \quad (120)$$

$$\gamma_{rz} = \frac{3pr(h^2-4z^2)}{4Gh^3} \quad (121)$$

Studies showed that the stress expressions obtained by this solution is the same as the ones obtained by the solution method presented in Barber [26].

It should be noted that for $\nu = 1/2$, the deflection expression becomes

$$w = \frac{P}{Gh^3}\left(-0.171875a^4 - 0.046875r^4 - 0.16h^3z - 0.375r^2z^2 + 0.375z^4 + h^2(0.21875r^2 - 0.3125z^2) + a^2(-0.21875h^2 + 0.21875r^2 + 0.4375z^2)\right) \quad (122)$$

2.3 One Dimensional Solution

The three dimensional elasticity equations reduce to one dimensional equations by several assumptions which are stated in Love-Kirchhoff Plate Theory. These assumptions are:

1. The thickness of the plate is small compared to the lateral dimensions. The normal stress in the transverse direction can be vanished compared to the normal stresses in the plane of the plate.

2. The deflection w of the plate is small compared to the plate thickness. The curvature of the plate after deformation can then be approximated by the second derivative of the deflection w.

3. The center plane of the plate is stress free, i.e., we can neglect the membrane stresses in the plate.

Using these assumptions, a one dimensional solution for the problem is be formulated in the following part.

2.3.1 Solution Presented in Timoshenko and Woinowsky-Krieger [8]

The differential equation for the uniformly loaded circular plate using Love-Kirchhoff Plate Theory is given by Timoshenko [8] as:

$$\frac{d}{dr}\left(r\frac{d}{dr}\left(r\frac{dw}{dr}\right)\right)=\frac{qr}{2D} \tag{123}$$

The above equation is a third order ordinary differential equation. After intrgrationg both sides three times, the deflection *w* may obtained. The following equation is obtained by the first integration:

$$\frac{1}{r}\frac{d}{dr}\left(r\frac{dw}{dr}\right)=\frac{qr^2}{4D}+C_1 \tag{124}$$

The second integration gives the following equation:

$$\left(r\frac{dw}{dr}\right)=\frac{qr^4}{16D}+\frac{C_1 r^2}{2}+C_2 \tag{125}$$

Finally, the third integration gives the deflection as:

$$w=\frac{qr^4}{64D}+r^2C_1+C_2\mathrm{Log}\left(\frac{r}{a}\right)+C_3 \tag{126}$$

The integration constants (C_1, C_2 and C_3) are obtained by using the boundary conditions of simply supported edge circular plate. These boundary conditions are:

1- Slope ($\theta = dw/dr$) of the deflection is zero at r=0, which implies:

$$\frac{dw}{dr}|_{r=0}=0$$

$$\frac{qr^3}{16D}+2rC_2+\frac{C_2}{r}=0 \quad (\text{at } r=0) \tag{127}$$

From the above equations, it can be concluded that $C_2=0$, as at r=0 C_2 should be equal to zero for a definite solution.

2- The deflection *w* at the edge of plate r=a is equal to zero. The following equation can be written using this condition:

$$w(a)=\frac{qa^4}{64D}+a^2C_1+C_3=0 \tag{128}$$

3- The magnitude of the radial moment is zero at the edge of the plate (r=a). This gives

$$M_r(a)=-D\left(\frac{d^2w}{dr^2}+\frac{\nu}{r}\frac{dw}{dr}\right)|_{r=a}=-D\left(\frac{3qa^2}{16D}+2AC_1+\frac{\nu\left(\frac{pa^3}{16D}+2aC_1\right)}{a}\right)=0 \tag{129}$$

where D is the modulus of rigidity (flexural rigidity) and equal to $Ez^3/12(1-\nu^2)$. By taking thickness equal to *h*, it becomes

$$D = \frac{E\,h^3}{12(1-\nu^2)} \tag{130}$$

Solving Eqs. (128) and (129) for the constants C_1 and C_3, the following results are obtained:

$$C_1 = -\frac{a^2 q(3+\nu)}{32D(1+\nu)} \tag{131}$$

$$C_3 = \frac{a^4 q(5+\nu)}{64D(1+\nu)} \tag{132}$$

Substituting C_2=0, and Eqs. (131) and (132) into Eq. (126) gives the final deflection as:

$$w = \frac{q(a^2-r^2)}{64\,D}\left(a^2\frac{(5+\nu)}{(1+\nu)} - r^2\right) \tag{133}$$

The expressions of radial and tangential moments can be written as:

$$M_r = -D\left(\frac{d^2w}{dr^2} + \frac{\nu}{r}\frac{dw}{dr}\right) = D\left(\frac{d\theta}{dr} + \frac{\nu}{r}\theta\right) = \frac{q}{16}(a^2-r^2)\,(3+\nu) \tag{134}$$

$$M_\theta = -D\left(\frac{1}{r}\frac{dw}{dr} + \nu\frac{d^2w}{dr^2}\right) = D\left(\frac{\theta}{r} + \nu\frac{d\theta}{dr}\right) = \frac{q}{16}\left(a^2(3+\nu) - r^2(1+3\nu)\right) \tag{135}$$

The radial displacement, moments, strains and stresses are calculated for simply supported edge circular plate based on the above deflection expression w. The radial displacement becomes:

$$u_r = -z\frac{dw}{dr} = -\frac{qrz(r^2(1+\nu) - a^2(3+\nu))}{16d(1+\nu)} \tag{136}$$

The maximum moments are equal at the center of plate which yields

$$M_r = M_\theta = \frac{1}{16} a^2 q(3+\nu) \tag{137}$$

Radial and tangential strains become

$$\epsilon_r = \frac{du_r}{dr} = \frac{qz\left(-3r^2(1+\nu) + a^2(3+\nu)\right)}{16d(1+\nu)} \tag{138}$$

$$\epsilon_\theta = \frac{u_r}{r} = -\frac{qz\left(r^2(1+\nu) - a^2(3+\nu)\right)}{16d(1+\nu)} \tag{139}$$

Radial and tangential stresses can be obtained as

$$\sigma_r = \frac{E}{1-\nu^2}(\epsilon_r + \nu\epsilon_\theta) = -\frac{3\,q\,z(a^2 - r^2)\,(3+\nu)}{4h^3} \tag{140}$$

$$\sigma_\theta = \frac{E}{1-\nu^2}(\epsilon_\theta + \nu\,\epsilon_r) = \frac{3\,q\,z\left(-a^2(3+\nu) + r^2(1+3\nu)\right)}{4h^3} \tag{141}$$

The maximum radial and tangential stresses are at the center of the top of plate (z=h/2). They are

$$\sigma_r = \sigma_\theta = -\frac{3a^2 q(3+\nu)}{8h^2} \tag{142}$$

As in previous derivations, due to symmetry, $\tau_{r\theta}$, $\epsilon_{r\theta}$ and $M_{r\theta}$ are all equal to zero.
It should also be noted that for $\nu = 1/2$, the deflection expression becomes.

$$w = \frac{(0.0574a^2 - 0.015625r^2)q[a^2 - r^2]}{D} \tag{143}$$

The analytical results that are obtained by different solution methods presented in this chapter are compared with each other in the next chapter. In addition, these results will be compared with numerical results.

CHAPTER III

NUMERICAL RESULTS

3.1 General

The analytical three dimensional and one dimensional solutions of the uniformly loaded simply supported circular plate problem were presented in Chapter II. In this chapter, some numerical results containing the stresses, strains and displacements will be given. In the first part, the distributions of the stresses, strains and displacements obtained by the two analytical methods are presented for different plate thicknesses. Then, the details of SAP 2000 model will be presented. The comparisons of the numerical results with the analytical results will be presented at the end of the chapter.

In the comparison studies, the radius of the plate is taken as a=100 mm, and the intensity of the uniform load which is applied on the top of the plate is taken as p=0.12 MPa. The material properties which are used in the analyses are given in Table 3.1. The h/a ratios for the plates considered in the analyses are taken as 1/5, 1/10, 1/20 and 1/40. These values correspond to plate thicknesses of 20 mm, 10 mm, 5 mm and 2.5 mm, respectively.

Table 3.1 Mechanical properties of the material used in the solutions

E (MPa)	ν	G (MPa)
5600	0.15	2434.7

3.2 Analytical Solutions

3.2.1 Three Dimensional Solution

The stresses, strains and displacements obtained by using the three dimensional solution is presented in this part.

3.2.1.1 Distribution of Stresses

The distribution of the radial, tangential, shear and transverse stress are computed using the corresponding equations at Chapter II based on the material properties given above. It is found that the two three dimensional solutions give identical results. Due to this reason, results obtained by Timoshenko et al. [7] will be presented.

The distributions of radial stress (σ_r) at the top of the plate (z=h/2) for different h/a ratios are given in Fig. 3.1 based on Eq. (112). The radial stress is maximum at the centre (r=0) of the plate, while its value at the edge of the plate (r=a) is zero, as shown in this figure.

In view of Eq. (113), the tangential stress (σ_θ) at the top of the plate (z=h/2) for different h/a ratios are shown in Fig. 3.2. It's obvious that the maximum tangential stress is at the centre of the plate (r=0) and its maximum intensity changes as the thickness of the plate changes. It should also be noted that the tangential stress is nonzero at r=a.

The distribution of transverse normal stress (σ_Z) along the height of the plate is shown in Fig 3.3. As seen in Eq. (114), the transverse normal stress does not depend on radial coordinate r. Due to this reason, its distribution along the thickness of the plate is presented only for h=20mm. The transverse normal stress (σ_Z) is maximum at the top of the plate (z=10 mm), zero at the neutral axis and minimum ($\sigma_Z = 0$) at the bottom (z=-10 mm). It should be noted that the stress distribution is symmetric

with respect to the neutral axis and the value of the stress at the top of the plate is equal to the uniform load intensity *p*.

Finally, the variation of shear stress (τ_{rz}) with radius for h=20 mm is presented in Fig.3.4. The minimum shear stress (τ_{rz}) is zero at the top and bottom of the plate (z=10 mm, z=-10 mm) and satisfy the boundary conditions, while the maximum value of shear stress is calculated at the edge of the middle plate (z=0, r=100 mm).

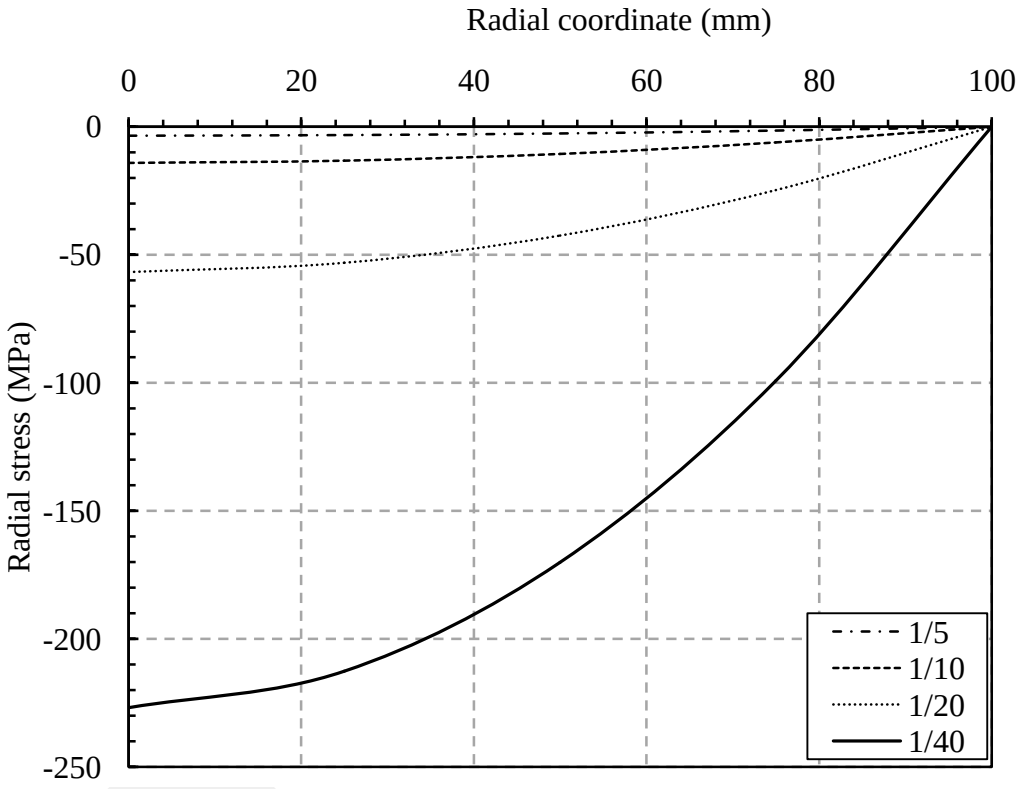

Fig. 3.1 The distribution of radial stress (σ_r) for different h/a ratios (1/5, 1/10, 1/20, 1/40)

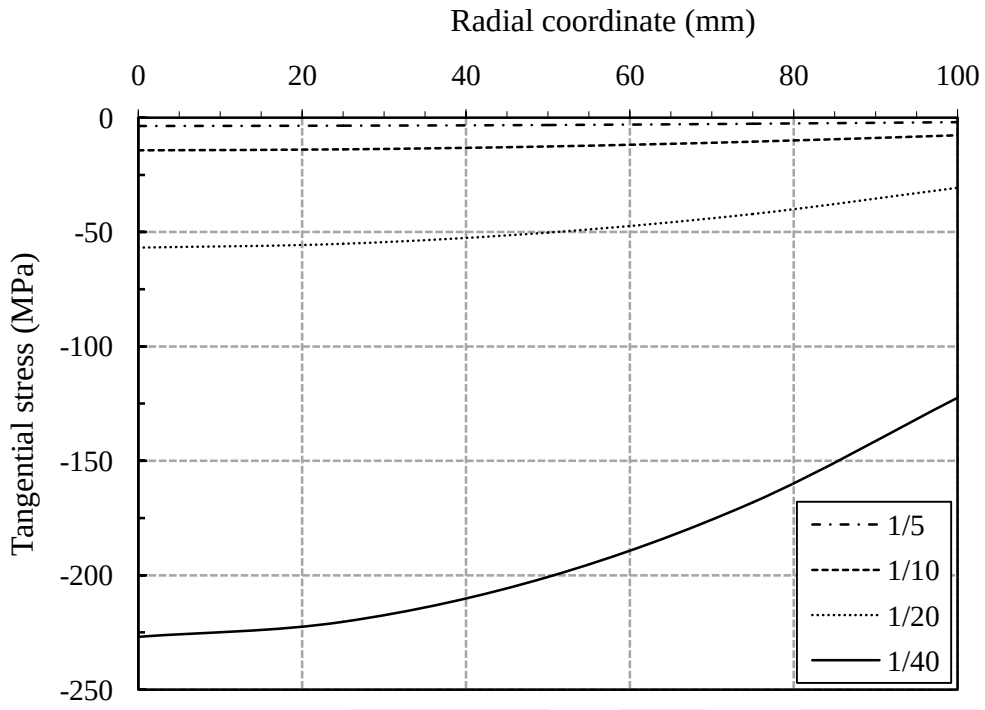

Fig. 3.2 The distribution of tangential stress (σ_θ) for different h/a ratios (1/5, 1/10, 1/20, 1/40)

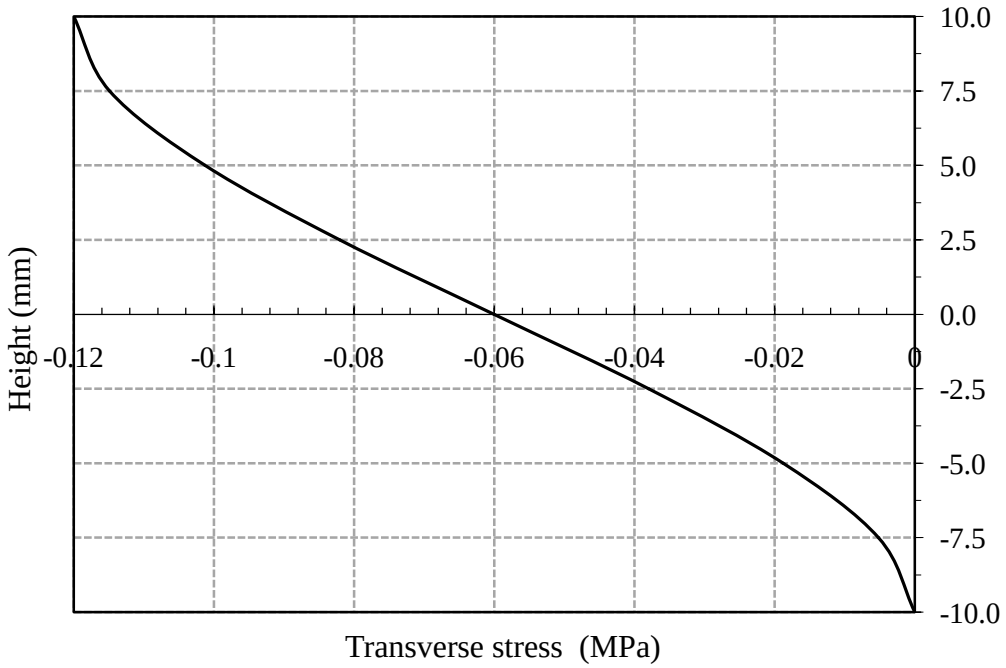

Fig. 3.3 The distribution of transverse stress (σ_Z) for thickness h=20 mm at the center of plate (r=0)

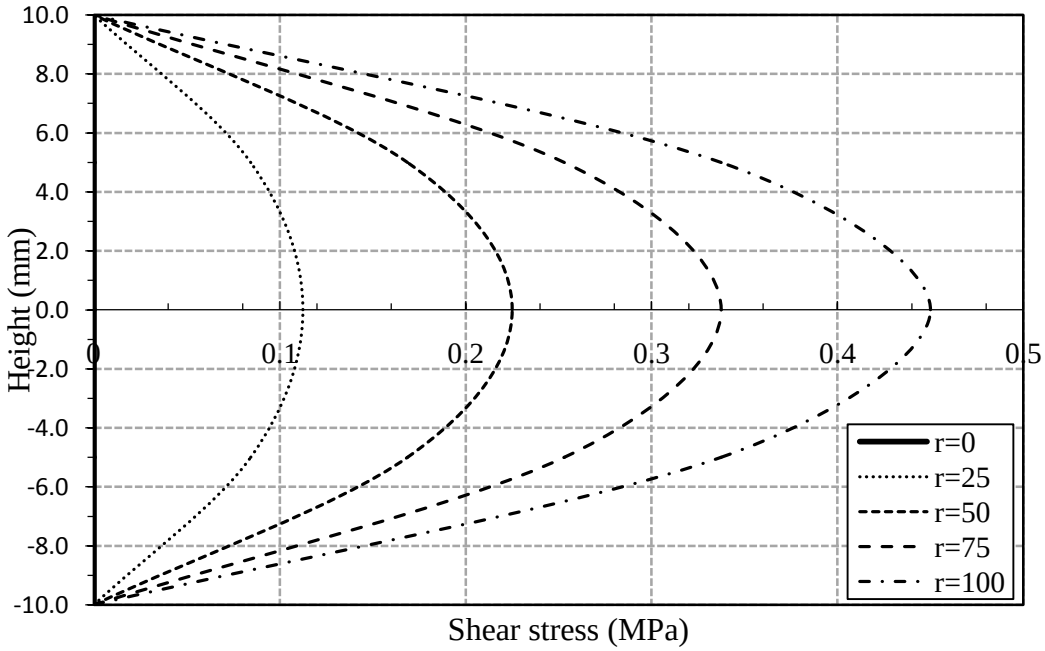

Fig. 3.4 The distribution of shear stress (τ_{rz}) for thickness h=20 mm for different radial coordinates

3.2.1.2 Distribution of Strains

The radial, tangential, transverse and shear strain distributions are obtained by using Eqs. (118), (119), (120), and (121), which are derived in Chapter II. The maximum radial strain ϵ_r and tangential strain ϵ_θ are obtained at the centre of the plate and their maximum value depend on the (h/a) ratio. By increasing this ratio the radial strain ϵ_r and tangential strain ϵ_θ increase as shown in Fig. 3.5 and Fig. 3.6. The distributions of shear strain γ_{rz} for different radial coordinates are shown in Fig.3.7. These distributions are similar to the distribution of the shear stress τ_{rz}. The maximum value of shear strain is calculated at the edge of the middle plane (z=0, r=100 mm). Finally, the transverse normal strain ϵ_z is calculated at the top of the plate (z=h/2) for different (h/a) ratios according to Eq. (120) and presented in Fig. 3.8.

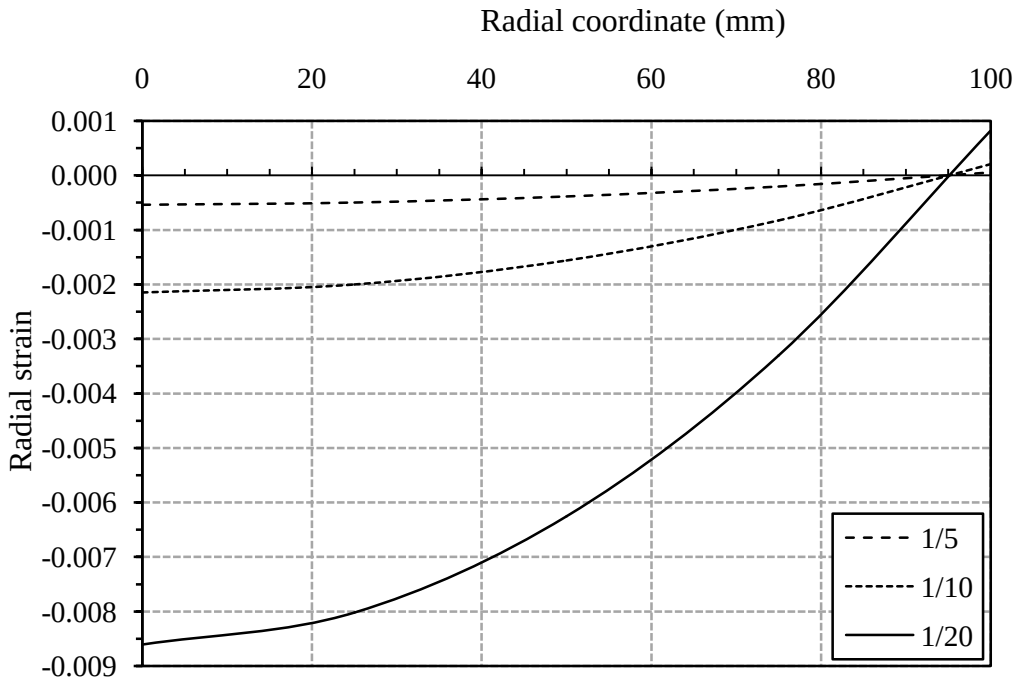

Fig. 3.5 The distribution of radial strain (ϵ_r) at the top of the plate (z=+h/2) for different h/a ratios (1/5, 1/10 and 1/20)

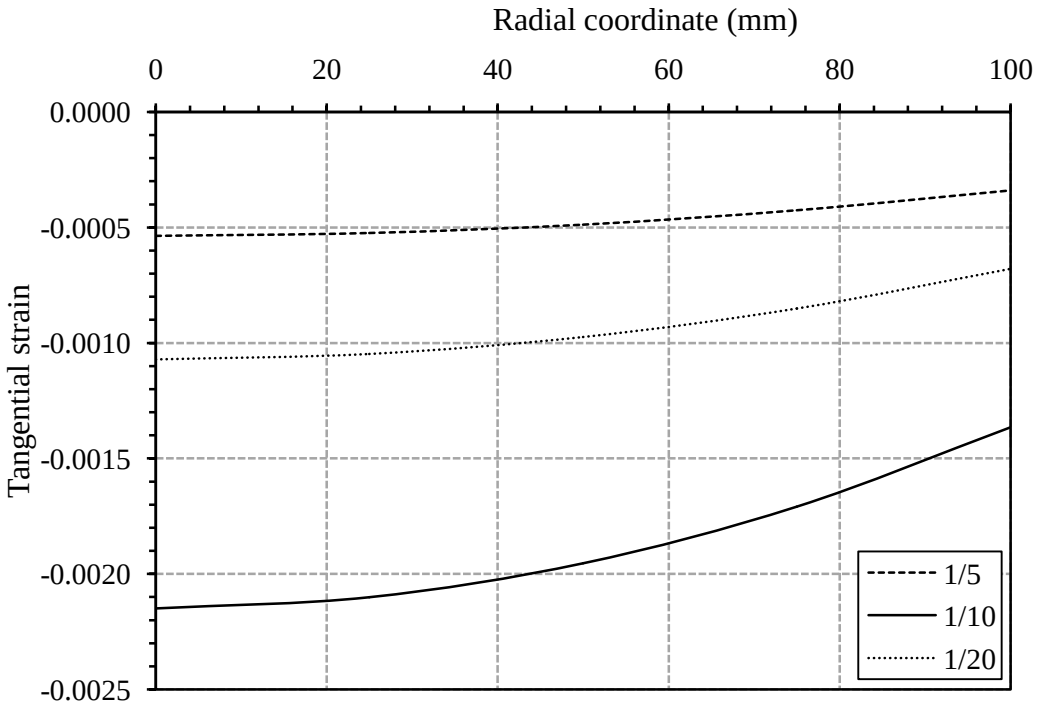

Fig. 3.6 The distribution of tangential strain (ϵ_θ) at the top of the plate (z=+h/2) for different h/a ratios (1/5, 1/10 and 1/20)

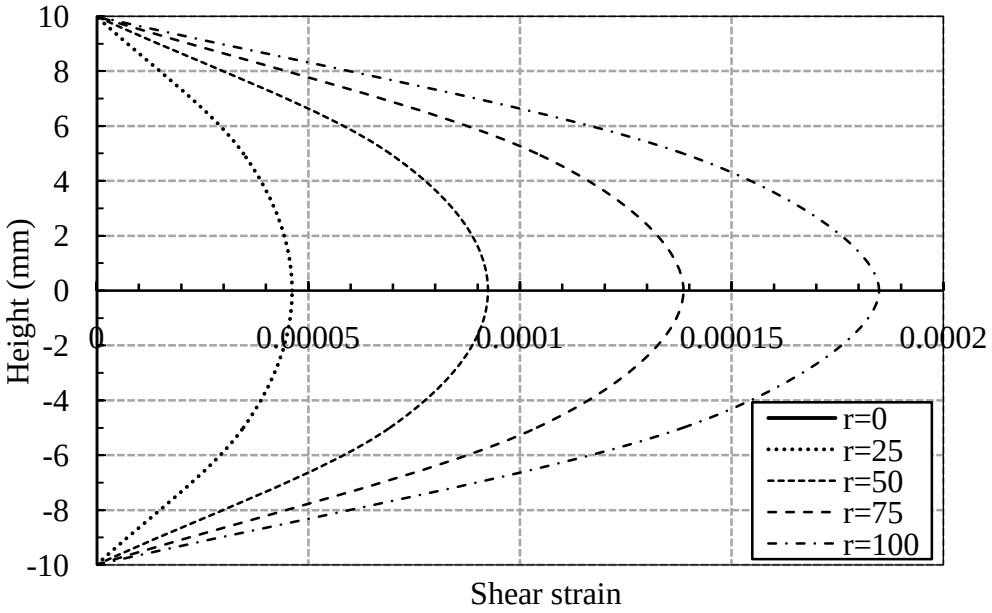

Fig. 3.7 The distribution of shear strain (γ_{rz}) at the top of the plate (z=+h/2) at different radial coordinates

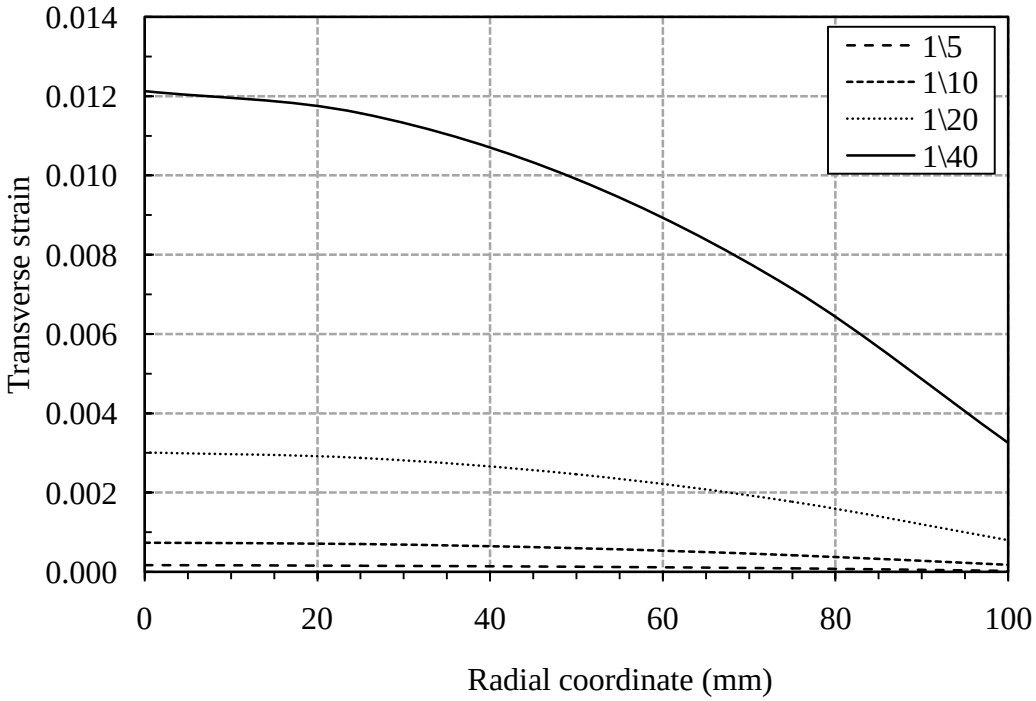

Fig. 3.8 The distribution of transverse strain (ϵ_z) at the top of the plate (z=+h/2) for different h/a ratios (1/5, 1/10, 1/20 and 1/40)

3.2.1.3 Distribution of Displacements

Transverse displacement (*w)* and radial displacement *(u)* are obtained numerically for different plate h/a ratios based on the Eqs. (117) and (116), respectively. The deflection (*w)* is maximum at the centre of the plate, while its value approaches to zero at the edge of the plate as shown in Fig. 3.9.

The distribution of the radial displacement (*u*) is completely different from the distribution of the deflection (w). Its maximum value is at the edge of the plate and it is equal to zero at the centre of the plate as shown in Fig. 3.10.

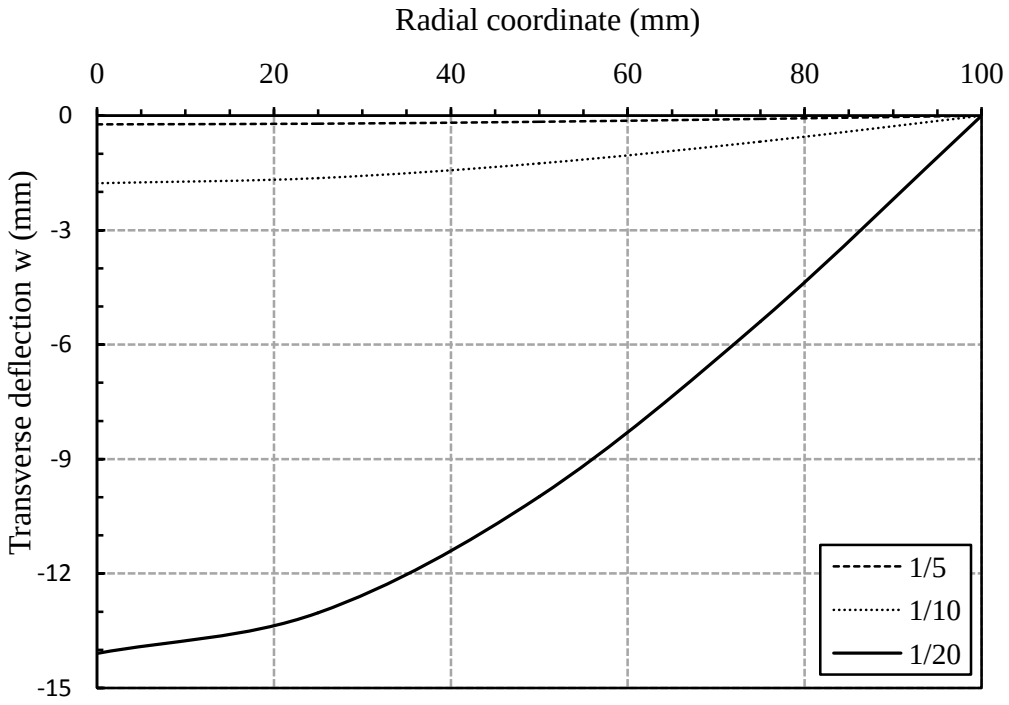

Fig. 3.9 The distribution of the deflection (*w*) at the top of the plate (z=+h/2) for different h/a ratios (1/5, 1/10 and 1/20)

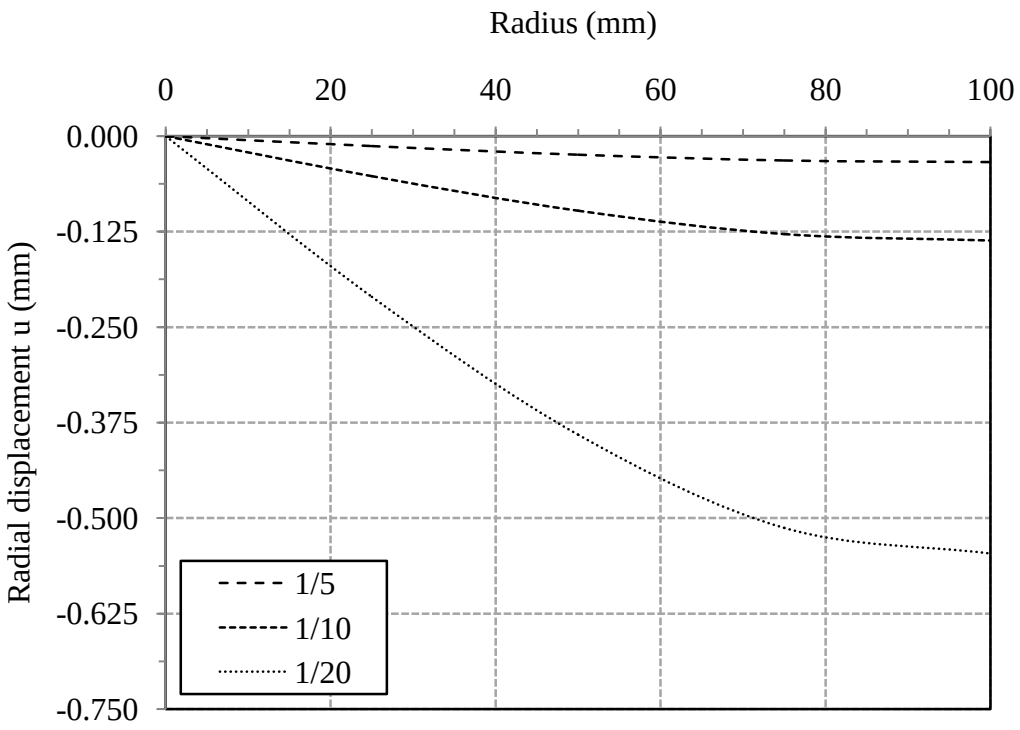

Fig. 3.10 The distribution of the radial displacement (*u*) at the top of the plate (z=+h/2) for different h/a ratios (1/5, 1/10 and 1/20)

3.2.2 One Dimensional Solution

Stress, strain and displacements for one dimensional solution are obtained for the middle surface (z=0). In the next part, these results will be presented.

3.2.2.1 Distribution of Stresses

Using Eqs. (140) and (141) the radial and tangential stress distributions according to one dimensional solution may be obtained. These stresses are illustrated in Fig.3.11. and Fig.3.12 for different plate thicknesses.

3.2.2.2 Distribution of Strains

Radial and tangential strain distributions based on one dimensional solution are obtained by using Eqs. (138) and (139). These results are illustrated in Figs.3.13 and 3.14.

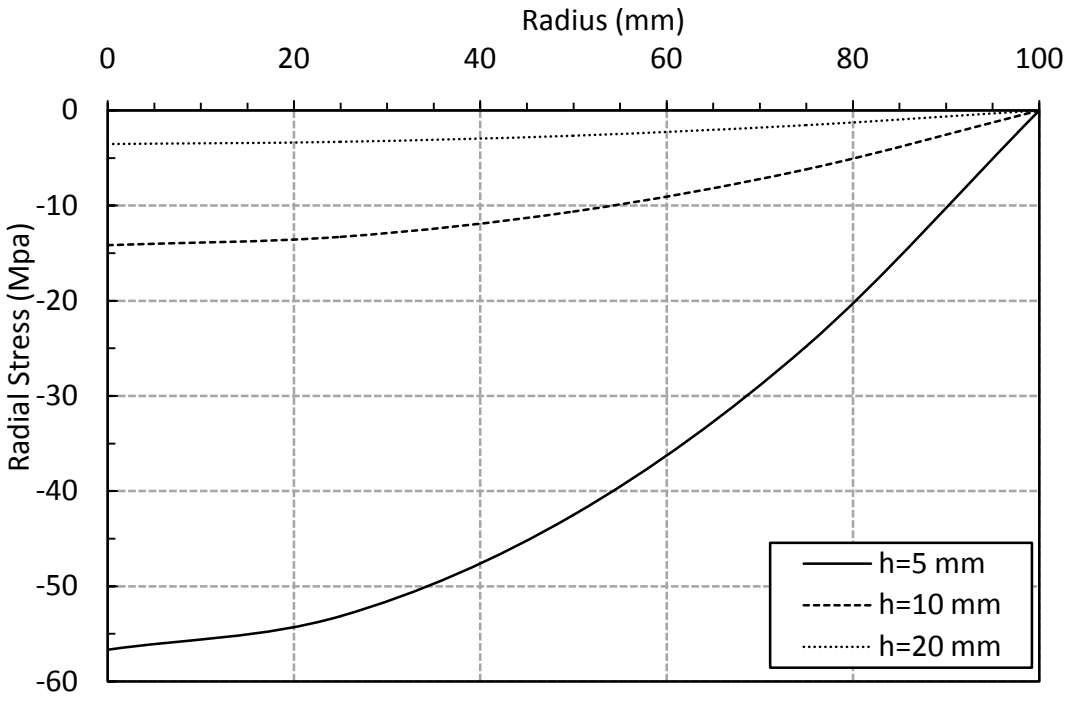

Fig. 3.11 The distribution of radial stress (σ_r) obtained by one dimensional solution for different plate thicknesses

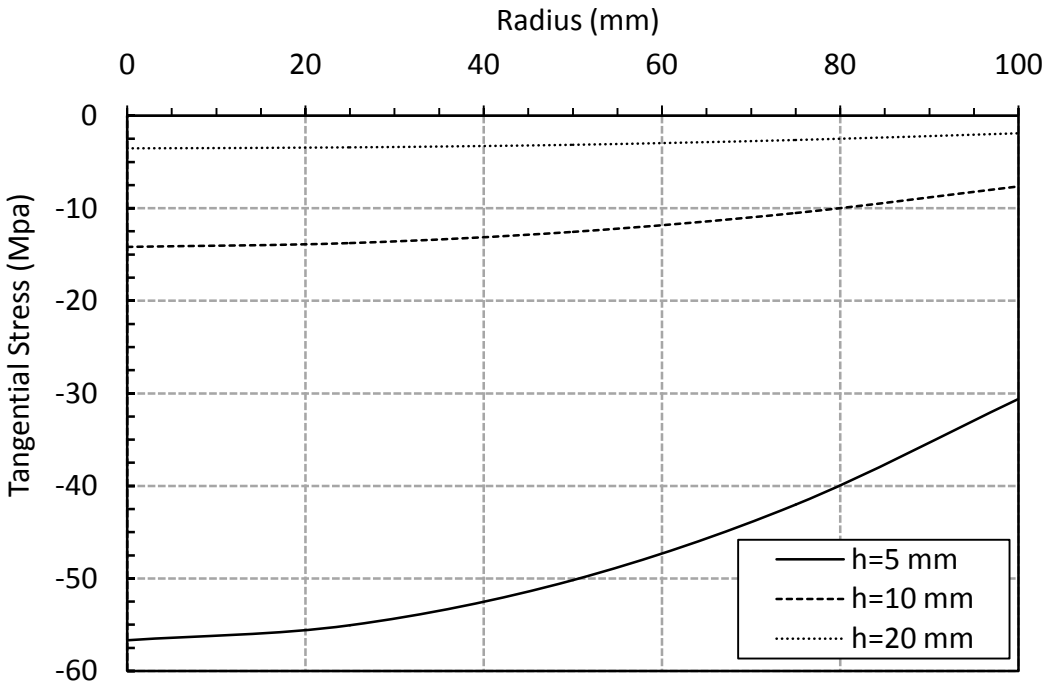

Fig. 3.12 The distribution of tangential stress (σ_θ) obtained by one dimensional solution for different plate thicknesses

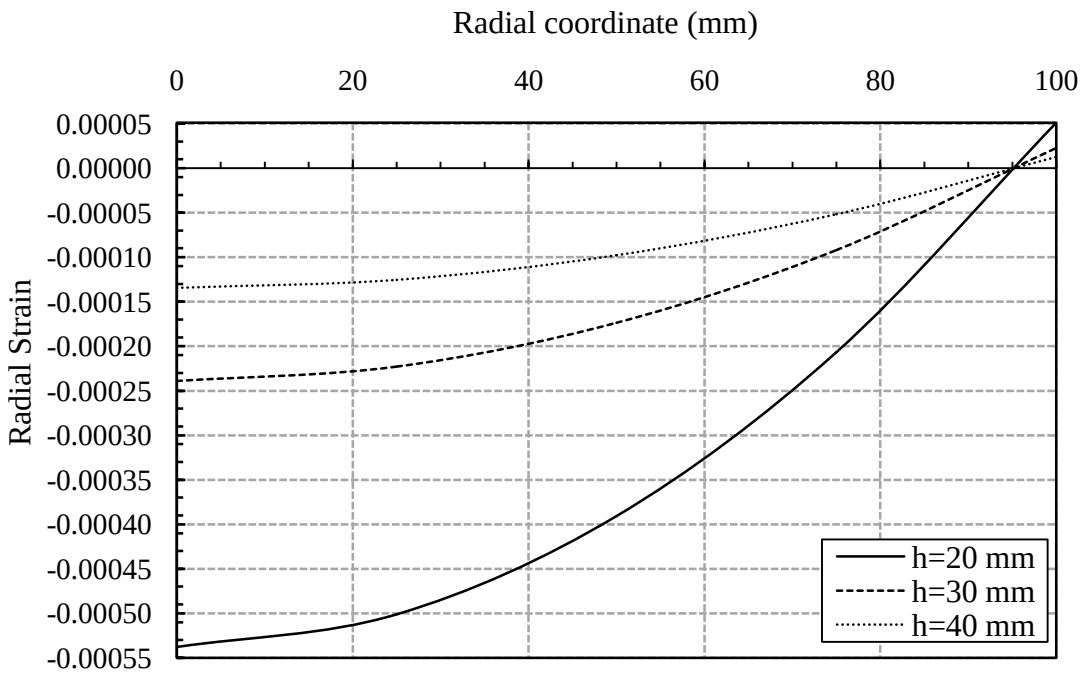

Fig. 3.13 The distribution of radial strain (ϵ_r) obtained by one dimensional solution for different plate thicknesses

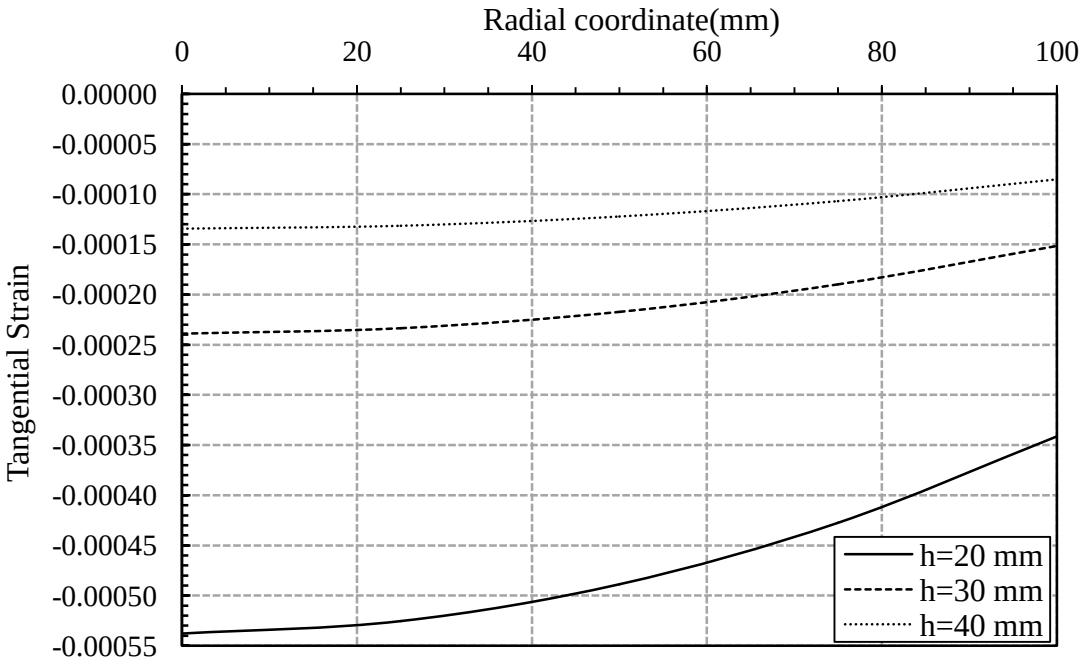

Fig. 3.14 The distribution of tangential strain (ϵ_θ) obtained by one dimensional solution for different plate thicknesses

3.2.2.3 Distribution of Displacements

Transverse and radial displacement distributions based on one dimensional solution are obtained by using Eqs. (143) and (136). The results are illustrated in Fig. 3.15 and Fig. 3.16.

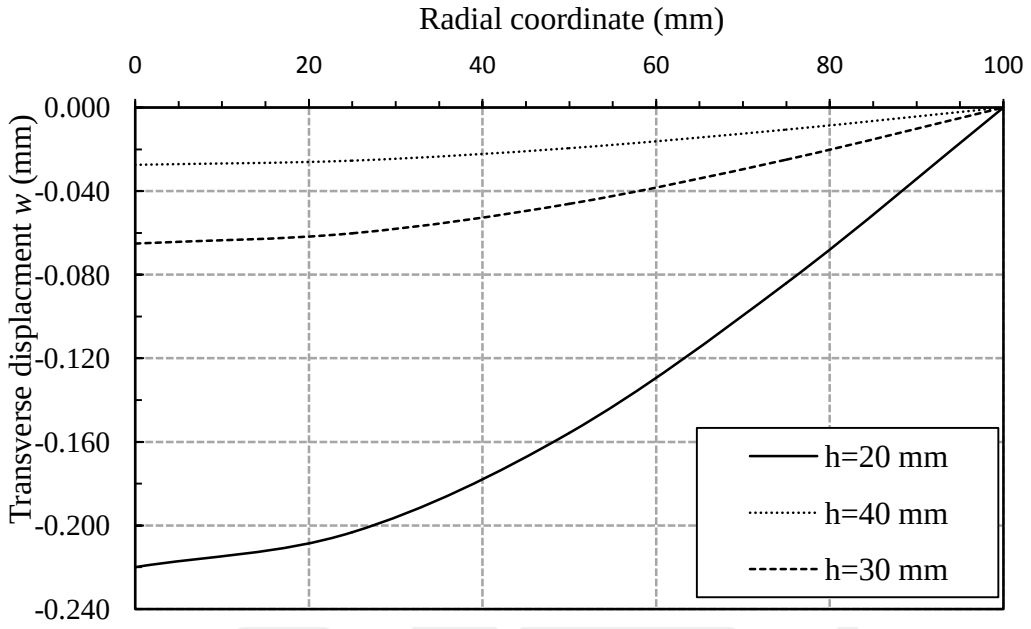

Fig. 3.15 The distribution of deflection (w) obtained by one dimensional solution for different plate thicknesses

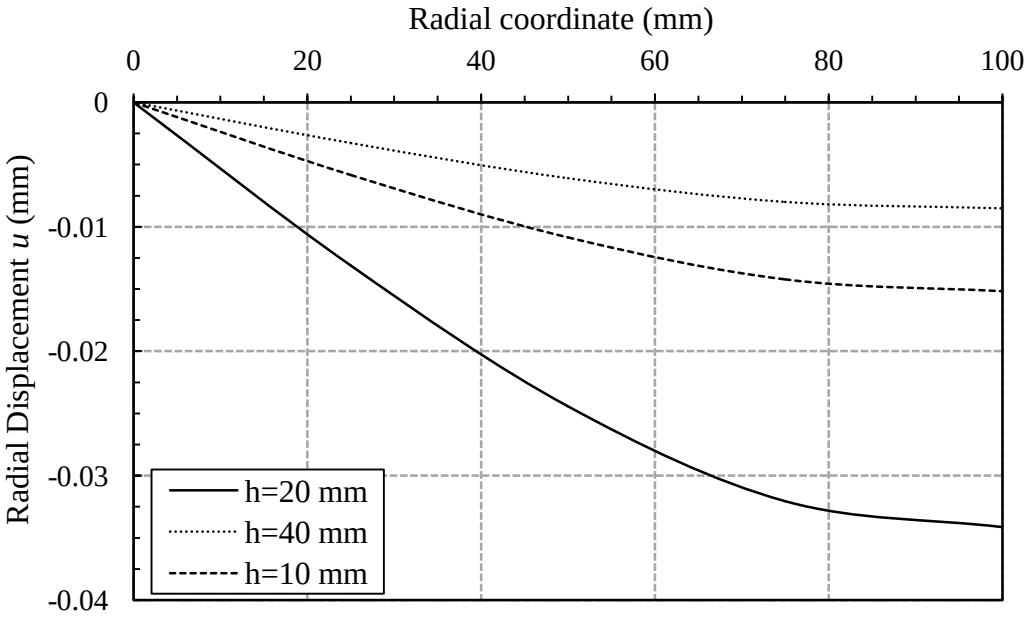

Fig. 3.16 The distribution of radial displacement (u) obtained by one dimensional solution for different plate thicknesses

3.2 Thin And Thick Plates

The circular plates can be classified for the sake of calculation into two classes: Thin and thick plates. For thin plates, one dimensional solutions can be used frequently because of the small thickness, while for the thick plates, the use of three dimensional elasticity approach might be required. It should be noted that the shear stresses and shear strains vanish for one dimensional solution. The effect of plate thickness on the shear stress and shear strain distributions is investigated for the circular plates in this part.

The distribution of the shear stress (τ_{rz}) and shear strain (γ_{rz}) for different plate thicknesses (5 mm, 10 mm, 20 mm, 40 mm) are shown in Figs. 3.17 and 3.18, respectively. It is seen from Fig.3.17 that, the maximum shear stress (τ_{rz}) changes as plate thickness changes. By increasing the thickness of the plate, the value of the shear stress may be decreased.

The distributions of the shear strain (γ_{rz}) for different thicknesses given in Fig 3.18 are similar to the distribution of the shear stress (τ_{rz}). It can also be concluded that by increasing the thickness of the plate, the shear deformations might be decreased.

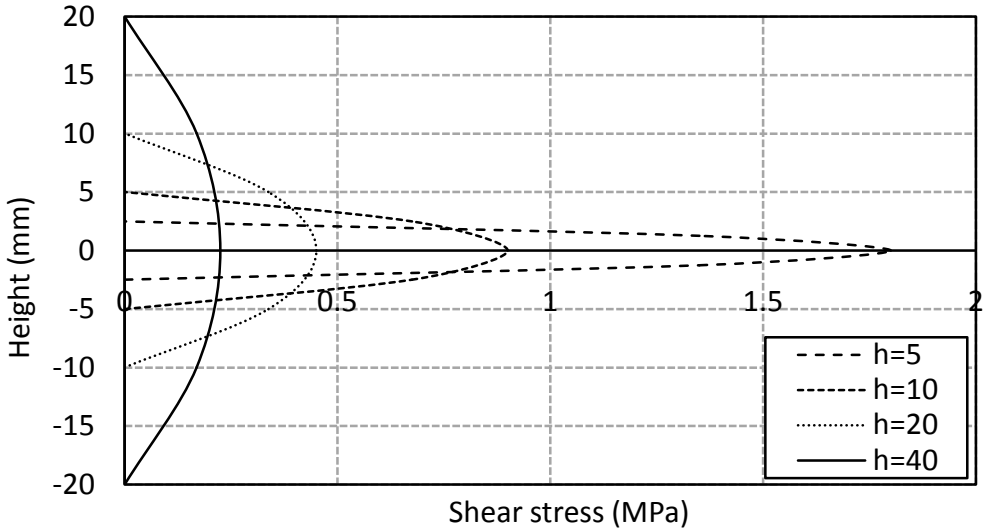

Fig. 3.17 The distribution of the shear stress (τ_{rz}) at the edge of middle plane of the plate (z=0) for different plate thicknesses (5 mm, 10 mm, 20 mm and 40 mm)

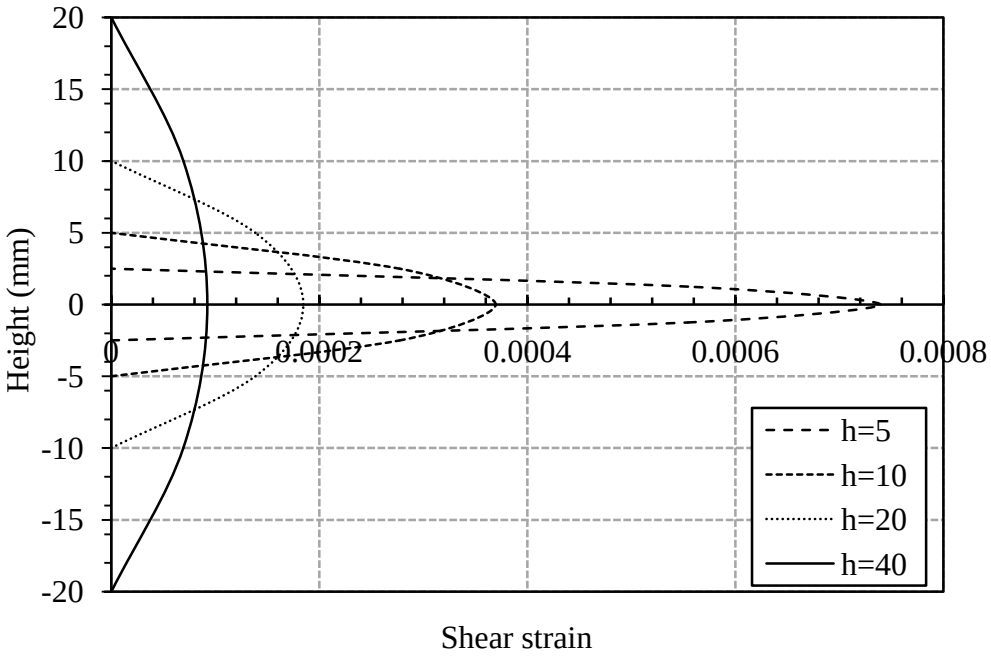

Fig. 3.18 The distribution of shear strains (γ_{rz}) at the edge of middle plane of the plate (z=0) for different plate thicknesses (5 mm, 10 mm, 20 mm and 40 mm)

The analytical results obtained by three and one dimensional approaches will be compared with the solutions obtained by the numerical method in the next part.

3.3 Numerical Solution

The circular plate under consideration is also modeled by SAP 2000 using two approaches based on the effect of the transverse shear deformation in the plate bending behavior. These two approaches are:

• The thick-plate (also called Mindlin/Reissner) formulation which takes into account the effects of transverse shear deformation

• The thin-plate (Classical or Kirchhoff) formulation, which neglects the effects of transverse shearing deformation

Shearing deformations are important when the thickness is greater than about one-tenth to one-fifth of the span. They can also be quite significant in the vicinity of bending stress concentrations, such as near sudden changes in thickness or support conditions, and near holes or re-entrant corners. Even for thin-plate bending problems, where shearing deformations are truly negligible, the thick-plate formulation tends to be more accurate, although somewhat stiffer, than the thin plate formulation [27]. In this part, these two plate models are used to obtain the numerical solutions of the problem.

In order to obtain an adequate element mesh in modeling of circular plates by SAP 2000 program, an iterative study is performed by considering the same geometry (h=1 mm, a=100 mm) and loading but using different mesh sizes. The maximum deflections are obtained for these models and plotted in Fig. 3.19. It is found that the relative error between a 256 area element model and a 144 area element model is about 0.3% (which might be considered as a satisfying percentage that shows the convergence) for the maximum deflection. Due to this reason, a 256 area element model is used to model the circular plate (Fig. 3.20).

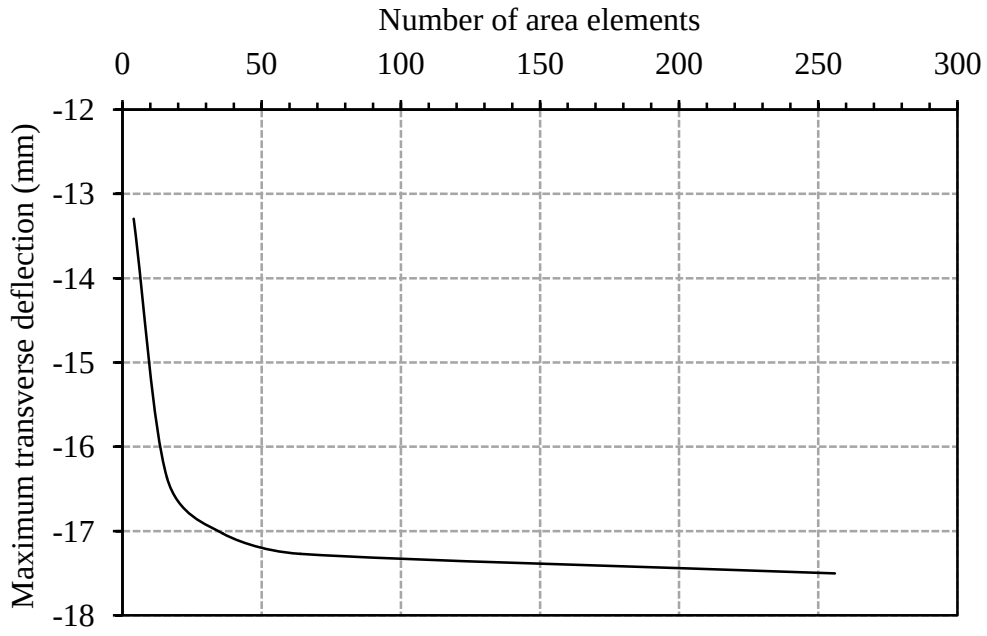

Fig. 3.19 Maximum transverse deflection obtained by different number of area elements

After determining the optimum number of elements to be used in the models, the uniformly distributed load of p=0.12 MPa is applied on the plate. The deflections are then obtained by using thin and thick plate assumptions. As an example, the deflection contour of a circular plate with h=20mm obtained using thin plate assumption is given in Fig. 3.21. In Fig. 3.22, the corresponding deformed shape of this circular plate is shown.

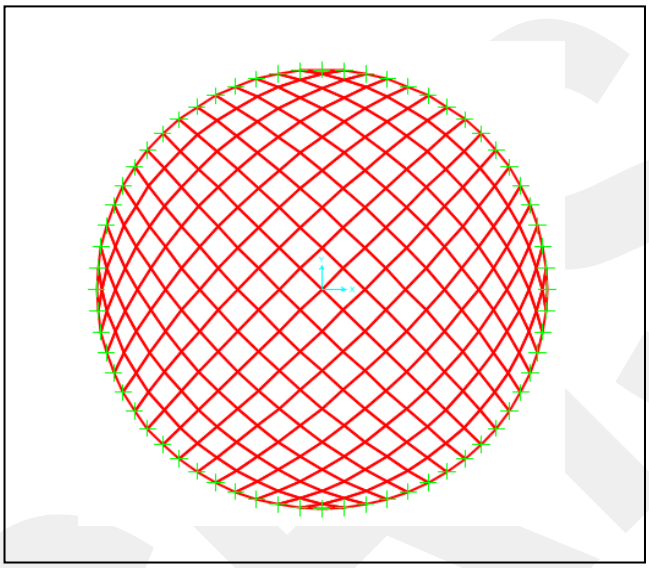

Fig. 3.20 The mesh of the circular plate model with 256 area elements

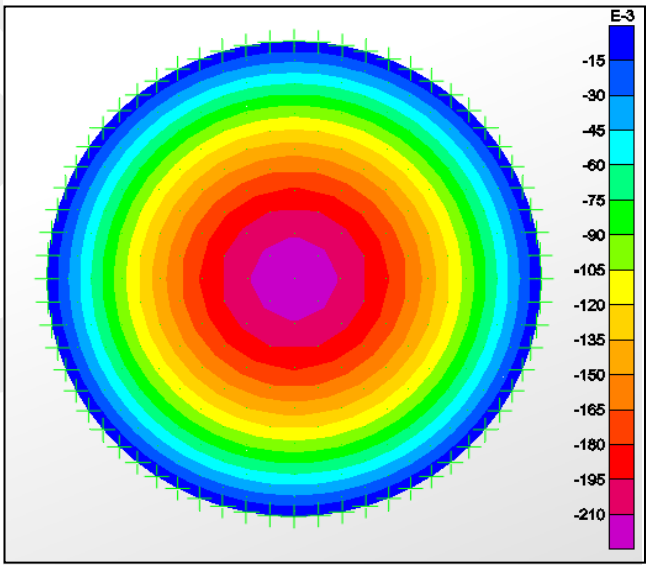

Fig. 3.21 Deflection contour (*w*) of a thin plate with thickness of 20 mm

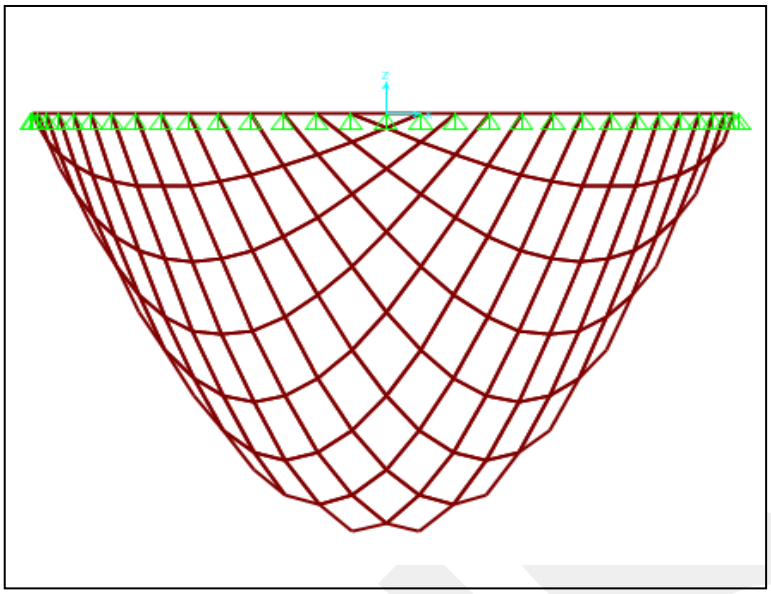

Fig. 3.22 Deflected shape of a thin plate with thickness of 20 mm

In the next part, the results obtained by analytical and numerical solutions are compared.

3.5 Comparison Studies

The results obtained by different approaches are compared with each other in this part. Firstly, the deflection (w) of the circular plate (a=100mm) under uniform loading is considered and the results obtained by (1) SAP 2000 thin elements, (2) SAP 2000 thick elements, (3) three dimensional solutions, and (4) one dimensional solution are compared. It is noticed that the deflections obtained by these four methods are close to each other if the thickness of the plate is taken as h=20 mm, as shown in Fig 3.23. The deflections become quite different if the thickness is increased to h= 60 mm as shown in Fig.3.24. This may be due to the thin plate assumption which neglects the transverse shear deformations. In order to clarify this concept, the relative difference between the maximum deflections for different plate thicknesses are evaluated and illustrated in Fig. 3.25. The deflections obtained by the three dimensional solution is considered to be the exact solution in the studies. The relative difference for the maximum deflection is calculated as 43% between the

three dimensional solution and SAP 2000 thin model and 5% between the three dimensional solution and SAP 2000 thick model. This value is 42.7% between the three and one dimensional solutions.

The distributions of radial stress obtained by one and three dimensional solutions are illustrated in Fig.3.26 for the plate thickness of h=40 mm. The radial stresses in this figure are based on Eqs. (140) and (112). On the other hand, the distributions of tangential stress for one and three dimensional solutions are shown in Fig. 3.27 for the same plate thickness. It is seen from both figures that, for this plate thickness the differences between the stresses are quite small. Figs. 3.28 and 3.29 show the distributions of radial and tangential strains for a plate with h=40 mm, which are obtained by one and three dimensional solutions. Similar to stresses, the strain distributions are close to each other. In order to identify the effect of plate thickness on the stresses and strains, the relative difference between one and three dimensional solutions for radial stress, tangential stress, radial strain and tangential strain are computed and illustrated in Figs. 3.30, 3.31, 3.32 and 3.33. As seen in these figures, the differences between two solutions become significant when the plate thickness is increased.

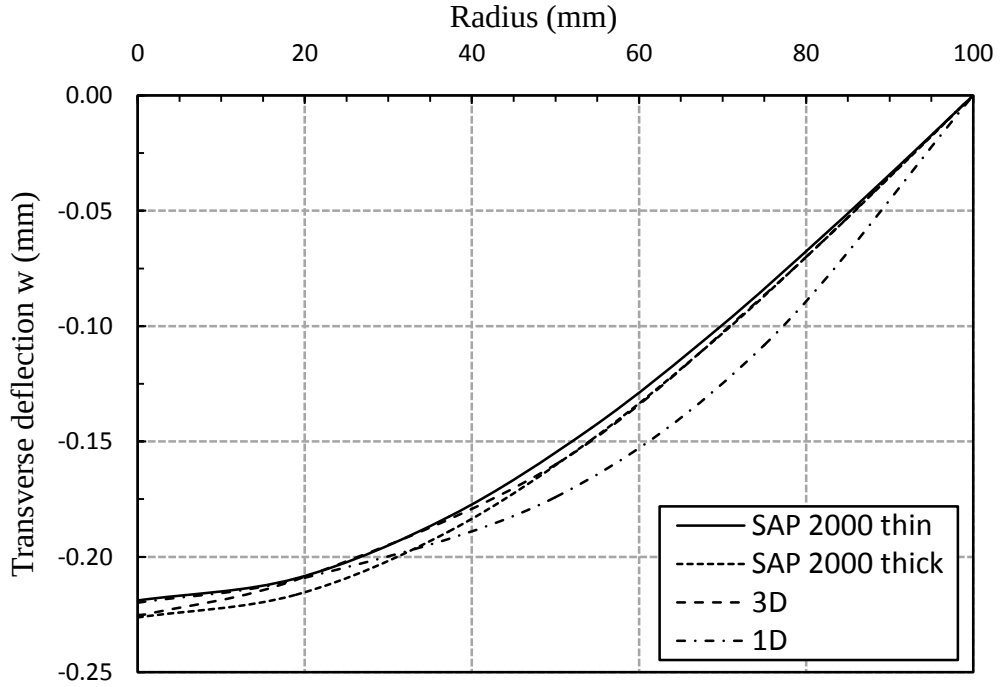

Fig. 3.23 The distribution of the deflection at the top of the plate (z= 10 mm) obtained by four methods

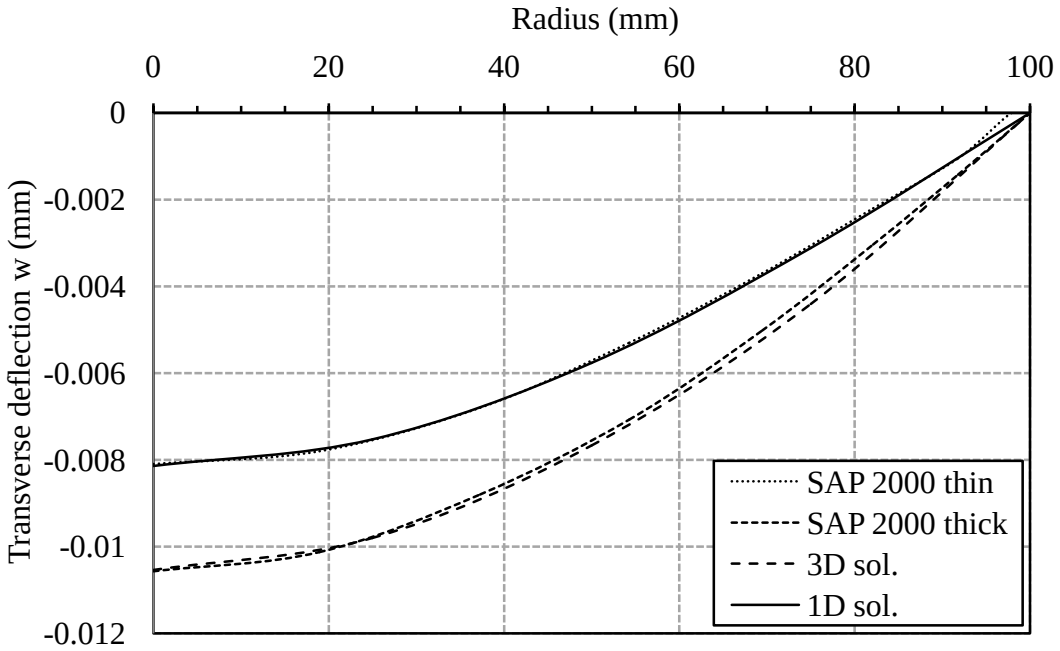

Fig. 3.24 The distribution of the deflection *(w)* at the top of the plate (z=30 mm) obtained by four methods

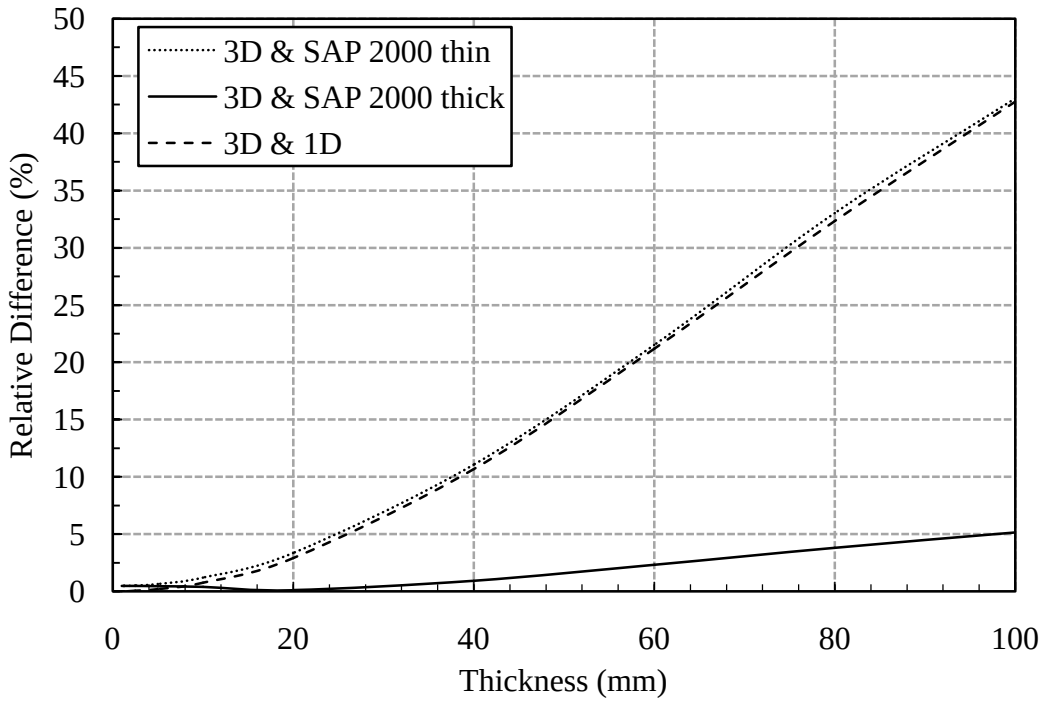

Fig. 3.25 Relative difference between the maximum deflections obtained by four methods for the thickness of a plate vary from 1 mm to 100 mm, a=100 mm

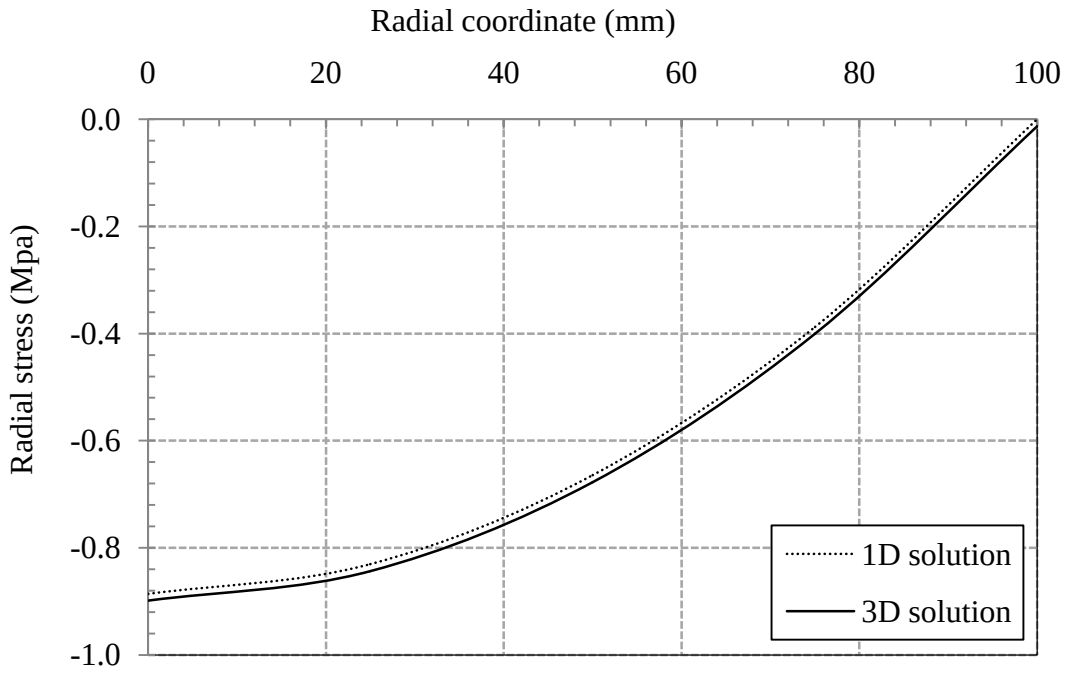

Fig. 3.26 The distribution of radial stress obtained by one and three dimensional solutions for plate thickness h= 40 mm

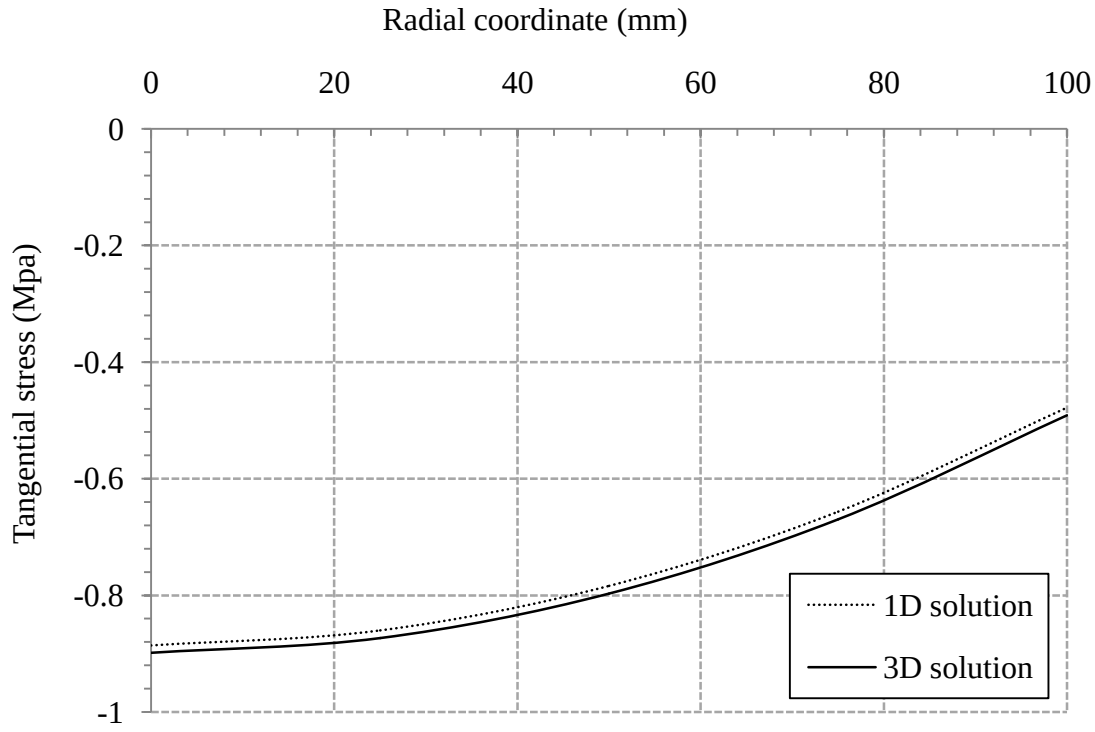

Fig. 3.27 The distribution of tangential stress obtained by one and three dimensional solutions for plate thickness h= 40 mm

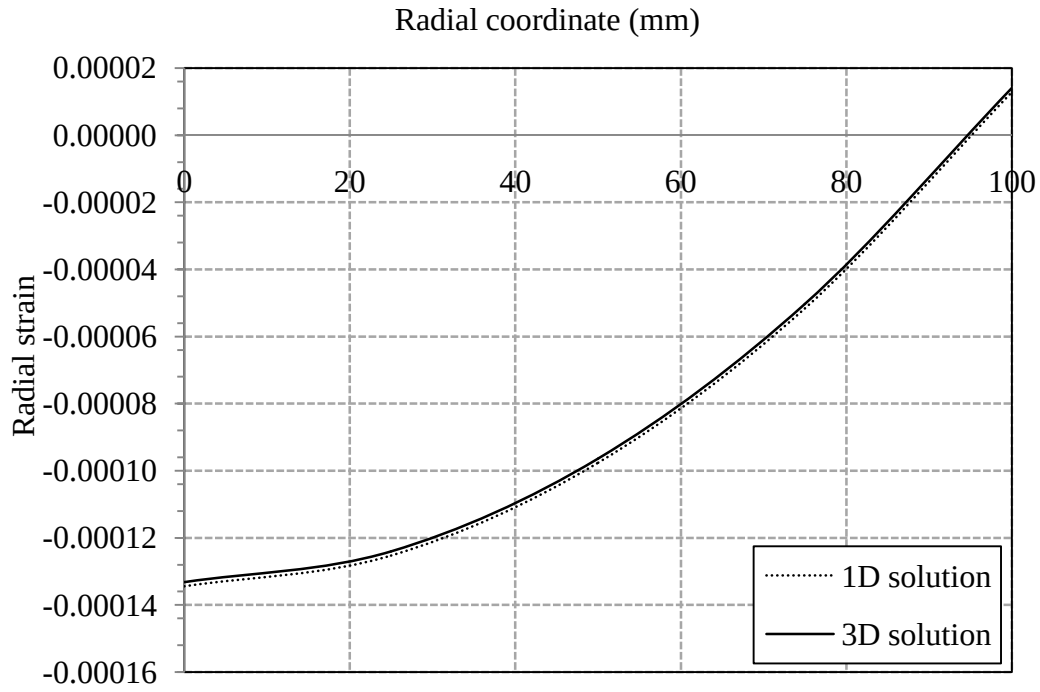

Fig. 3.28 The distribution of radial strain obtained by one and three dimensional solutions for plate thickness h= 40 mm

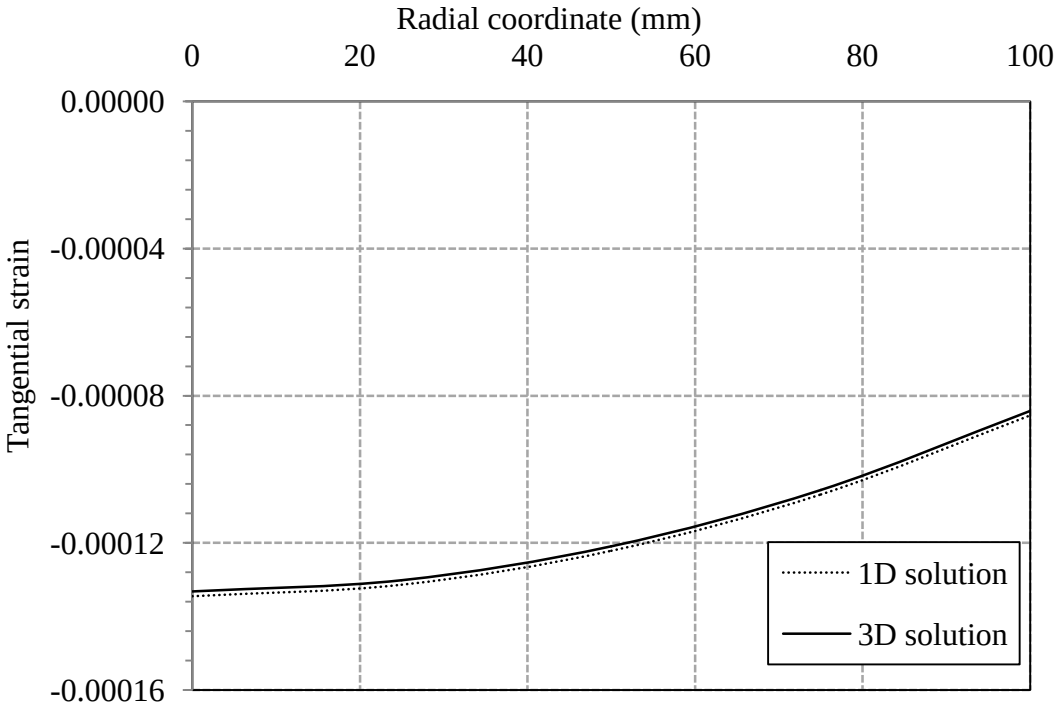

Fig. 3.29 The distribution of tangential strain obtained by one and three dimensional solution for plate thickness h= 40 mm

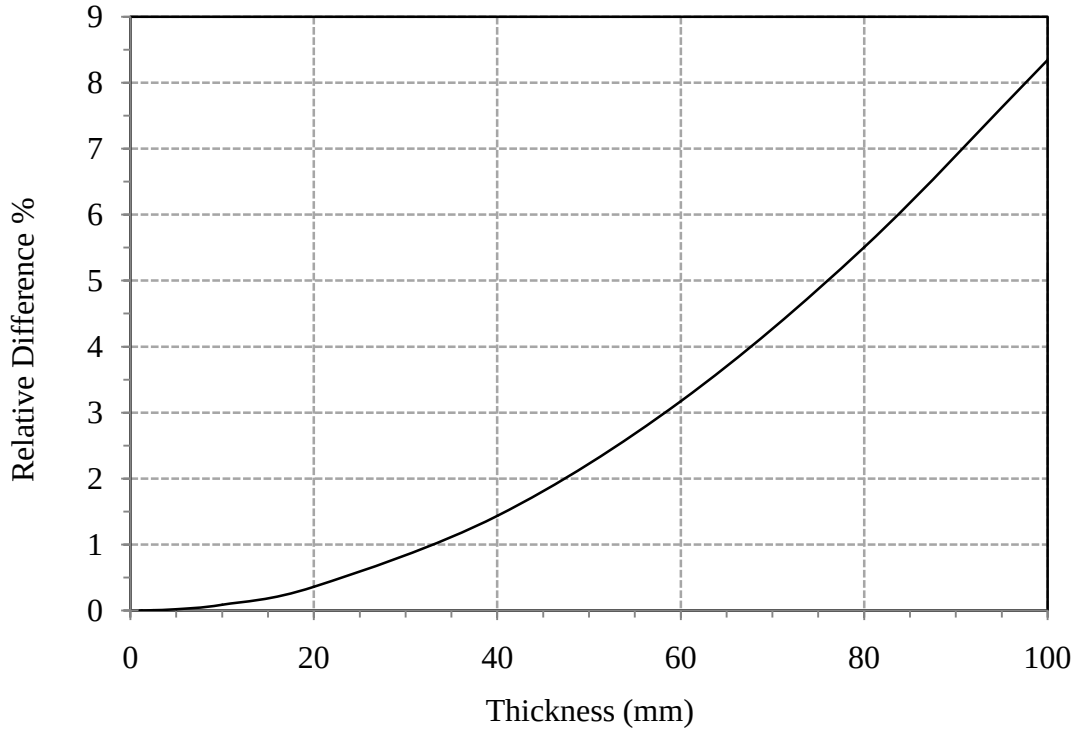

Fig. 3.30 Relative difference between maximum radial stresses obtained by one and three dimensional solutions for plate thicknesses vary from 1mm to 100mm, a=100mm

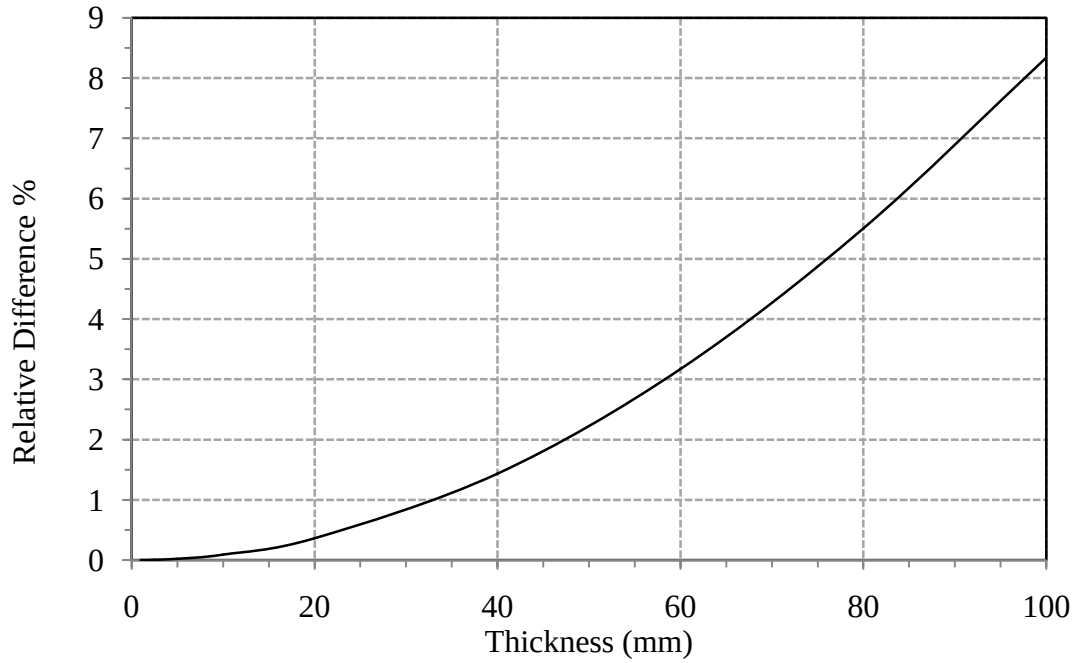

Fig. 3.31 Relative difference between maximum tangential stresses obtained by one and three dimensional solutions for plate thicknesses vary from 1mm to 100mm, a=100mm

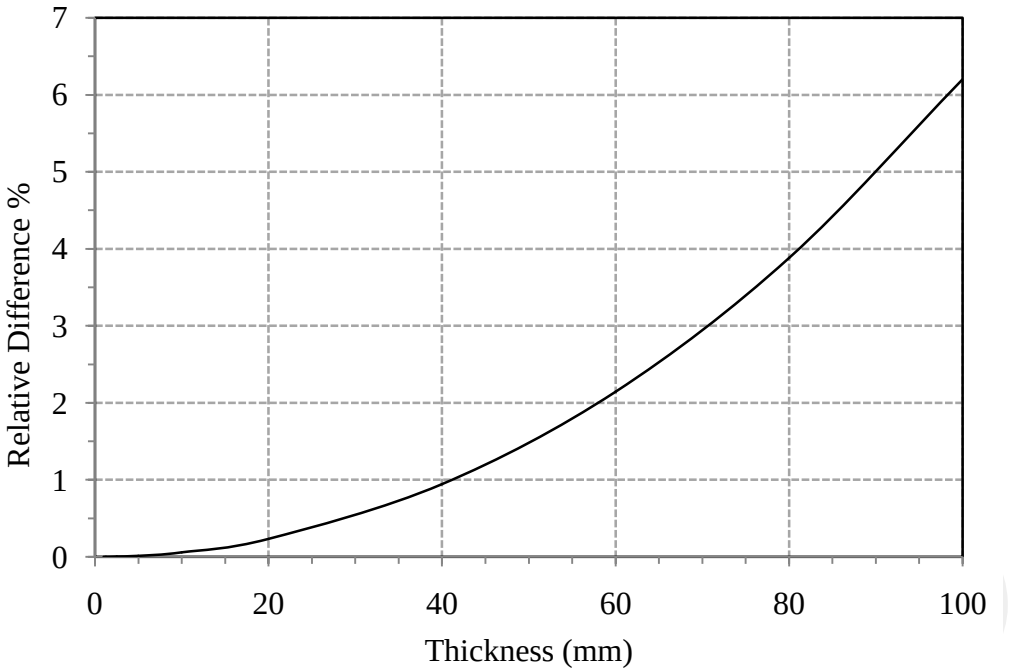

Fig. 3.32 Relative difference between maximum radial strains obtained by one and three dimensional solutions for plate thicknesses vary from 1mm to 100mm, a=100mm

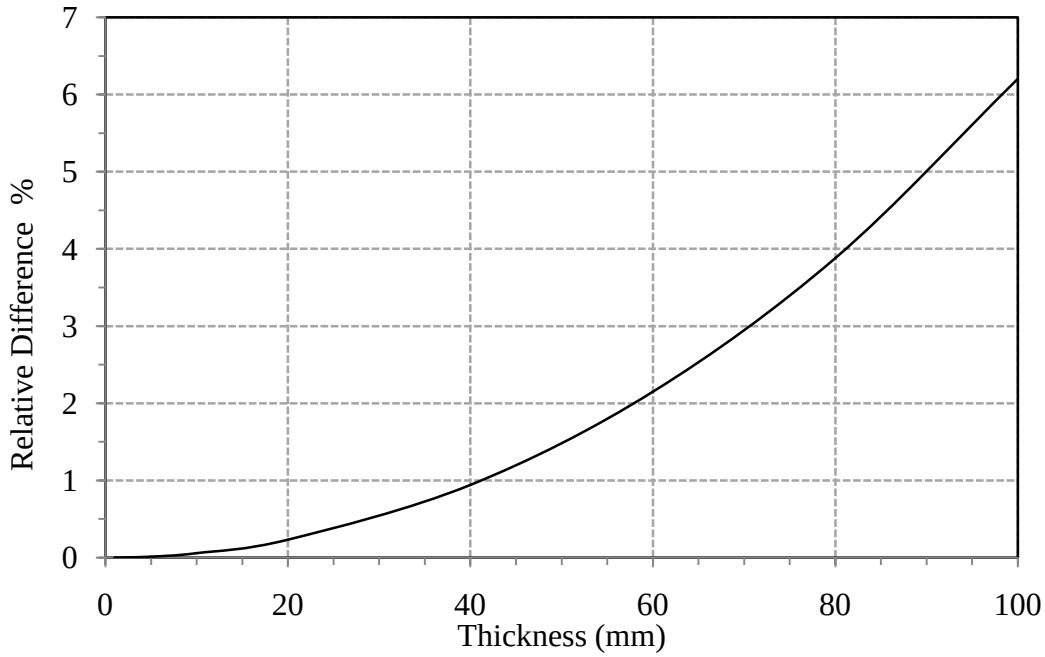

Fig. 3.33 Relative difference between maximum tangential strains obtained by one and three dimensional solutions for plate thicknesses vary from 1mm to 100mm, a=100mm

CHAPTER IV

SUMMARY AND CONCLUSION

In this study, the analytical solution of a simply supported circular plate under uniform loading is presented. Starting with a three dimensional approach based on the solution given by Barber [26], the expressions of the stresses, strains and displacements for the circular plate are derived. Later, a three dimensional solution based on Timoshenko and Goodier solution [7] is handled. Finally, a one dimensional solution of the problem is found by considering the solution presented by Timoshenko and Woinowsky [8]. Using these solutions, several numerical examples are handled in order to show the general behaviour of the circular plates under uniform loading. In the study, SAP 2000 program is also used in order to make comparisons between the results obtained from the analytical methods mentioned above and the finite element method.

Completing the involved algebra would have been impossible without the usage of the symbolic software, MATHEMATICA [6]. The use of symbolic software is useful for the study because it manipulates the given expressions and symbolically retains the variables. The method of selecting the polynomial which satisfies all the boundary conditions provides better accuracy and faster convergence. The use of the symbolic software provides much faster and accurate way of analyzing the engineering problems. With the examples illustrated in this thesis, it is evident that the results generated by the symbolic software shows good agreement with those of the finite element software, SAP 2000.

The following points are concluded in this study:

1- The stress, strain and displacement expressions obtained by the two three dimensional solutions are found to be identical. They are checked by MATHEMATICA and found to be the same.

2- Three dimensional solution is more accurate for thick plates, while one dimensional solution is suitable for only thin plates.

3- Relative difference between the results of the three and one dimensional solutions increases by increasing the thickness of the plate. This is due to neglecting the transverse shear in one dimensional solution.

4- The numerical results obtained by SAP 2000 thick plate elements are close to the results of the three dimensional solution. On the other hand, the solutions obtained by using SAP 2000 thin plate elements are close to the results of the one dimensional solution.

In this study the material properties used in the solution like modulus of elasticity and Poisson's ratio is constant along the plate and do not change with thickness or radius. For the future studies, this study may be used to develop analytical solutions for the two-layer or multi-layer circular plates with different boundary conditions and material properties. For instance, an orthotropic circular plate with functionally graded material properties may be analyzed using the three dimensional approach.

REFERENCES

[1] Szilard R., Theory and Analysis of Plates, Prentice-Hall Inc., Englewood Cliffs, New Jersey, 1974.

[2] Balasubramanian A., Plate analysis with different geometries and arbitrary boundary condition, MSc. Thesis, University of Texas at Arlington, 2011.

[3] Szilard R. Theory and Analysis of Plates: Classical and Numerical Methods, John Wiley and Sons Inc., New Jersey, 2004.

[4] Sokolnikoff I.S., Mathematical Theory of Elasticity (2nd Ed.), McGraw-Hill, N.Y., 1956.

[5] Nomura S., Wang B.P., Free vibration of plate by integral method, Computers and Structures, Volume 32, Issue 1, Pages 245-247, 1989.

[6] Stephen Wolfram, Mathematica: A System for Doing Mathematics by Computer. Redwood City, CA. Addison-Wesley, 1988.

[7] Timoshenko S.P., Goodier J.N., Theory of Elasticity (3rd Ed.), McGraw-Hill, New York, 1970.

[8] Timoshenko S.P., Woinowsky-Krieger S, Theory of Plates and Shells (2nd Ed.), McGraw-Hill, New York, 1959.

[9] Krauthammer E.V.T., Thin Plate and Shells, Marcel Dekker Inc., New York, 2001.

[10] Ugural A.C., Stresses in Plates and Shells, McGraw-Hill, New York, 1981.

[11] Ding H., Lee W. Y., Chen W.Q., Analytical solutions for uniformly loaded circular plate with clamped edges, Journal of Zhejiang University Science (6A), 1163-1168, 2005.

[12] Wang K., Analysis and calculation of stresses and displacements in layered elastic systems, Acta Mechanica Sinica, Vol.3, No.3, 251-260, 1987.

[13] Holzer H., Zeitschrift fur Turbinenwesen 15, 21, 1918.

[14] Olsson R.G., Biegung dreisformiger Platten von radial verander licher Steifigkeit, Ing. Archive 8, 81, 1937.

[15] Chakravorty J.G., Bending of symmetrically loaded circular plate of variable thickness, Indian Journal Pure Application Mathematics, Vol.11, No.2, 1980.

[16] Lee L.T., Lo W.K., Equivalent systems for variable thickness circular plates, Computer and Structures, Vol.58, No.5, 1996.

[17] Ghorashi M., Daneshpazhooh M., Limit analysis of variable thickness circular plates, Computer and Structures 79, 461-468, 2001.

[18] Saidi A.R., Jomehzadeh E., Atashipour S.R., Exact analytical solution for bending analysis of functionally graded annual sector plates, IJE Transactions, Vol.22, No.3, 2009.

[19] Yamanouchi M., Koizumi M., Hirai T., Shiota I., Proceedings of the 1st International Symposium on Functionally Gradient Materials. Functionally Gradient Materials Forum. The Society of Non-Traditional Technology, Japan, 1990.

[20] Koizumi M., Concept of FGM. Ceramic Trans. 34, 3-10., 1993

[21] Li X.Y., Ding H.J., Chen W.Q., Elasticity solution for a transversely isotropic functionally graded circular plate subject to an axisymmetric transverse load qr^k, International Journal of Solid and Structures 45, 191-210, 2008.

[22] Zheng L., Zheng Z., Exact solution for axisymmetric bending of functionally graded circular plate, Tsinghua Science and Technology, Vol. 14, Number 82, 2009.

[23] Zenkour A.M., A comprehensive analysis of functionally graded sandwich plates, Part 1-Deflection and stresses, International Journal of Solid and Structures 42, 5224-5242, 2005.

[24] Reddy J.N., Wang C.M., Kitipornachai S., Axisymmetric bending of functionally graded circular and annular plates, European Journal of Mechanics A/Solids 18, 185-199, 1999.

[25] Vrabie M., Baetu S., Comparative analysis of the bending theories for isotropic plates, Buletinul Institutului Politehnic Din Iaşı, Tomul LIX (LXII), Fasc. 3, 2013.

[26] Barber J.R., Elasticity (3rd Ed.), Springer Dordrecht Heidelberg, London-New York, 2010.

[27] SAP 2000 Integrated Finite Element Analysis and Design of Structures, BASIC ANALYSIS PEFERENCE (Chapter IV), 1995.